

**Empirically Optimized Landscape Resistance Reveals Barriers and
Facilitators of Gene Flow in Woodland Caribou**

Colin Warwick

Faculty of Natural Resources Management

Lakehead University

Thunder Bay, Ontario

September 15th, 2025

ABSTRACT

Understanding how landscape features shape genetic connectivity is critical for conserving wide-ranging species like woodland caribou (*Rangifer tarandus caribou*), particularly in managed landscapes where resource extraction and anthropogenic disturbance occur alongside natural disturbance. We used microsatellite genotypes from 244 individuals and four genetic distance metrics (Fij, Dps, PCA10, PCA64) to optimize resistance surfaces with ResistanceGA and assess spatial patterns of genetic structure in the Churchill Range, northwestern Ontario. Despite moderate genetic diversity (mean $H_e = 0.68$) and extremely low pairwise F_{ST} (< 0.003), spatial autocorrelation and clustering analyses indicated weak but significant genetic structure consistent with isolation by distance. Resistance modeling showed that isolation by distance alone provided a poor fit relative to models incorporating landscape features. Wetlands consistently emerged as the dominant predictor across three allele frequency-based metrics (DPS, PCA10, and PCA64), highlighting their role in sustaining broad-scale gene flow. In contrast, coniferous forest paired with water was the top predictor for kinship-based Fij, suggesting that conifer habitats influence genetic structure through more recent demographic processes such as philopatry and site fidelity. These results establish a genetic baseline for caribou in the Churchill Range and demonstrate that connectivity is shaped primarily by wetlands, with conifer habitats also contributing to more recent genetic structuring.

Keywords: woodland caribou, landscape genetics, gene flow, isolation by distance (IBD), isolation by resistance (IBR), population structure, habitat connectivity, wetlands, coniferous forest

ACKNOWLEDGEMENTS

I am deeply grateful to my supervisor, Dr. Ashley Thomson, for her guidance, support, and patience throughout this project. I also thank my lab mates, Hailey and Hannah, for their camaraderie and insight, and my girlfriend Caris for her constant encouragement. Finally, I owe much to my family and friends, whose support made this work possible.

Funding for this research was provided by the Ontario Ministry of the Environment, Conservation and Parks (MECP; award to A. Thomson) and by a Mitacs Accelerate scholarship (award to C. Warwick). I thank the contractors who collected field samples and acknowledge the use of AI tools (ChatGPT) for language refinement and code troubleshooting.

TABLE OF CONTENTS

INTRODUCTION	1
METHODS	6
Study Area.....	6
Sample Collection.....	7
DNA Extraction and Genotyping	9
Genetic Data Filtering and Quality Control	9
Genetic Distance and Spatial Autocorrelation	10
Genetic Diversity and Relatedness	11
Population Structure	12
Landscape Variables	13
Resistance Surface Modeling	14
RESULTS	16
Marker Quality Assessment	16
Genetic Structure and Diversity	16
Factors Affecting Gene Flow	21
DISCUSSION	24
Overview of Genetic Connectivity and Diversity	24
Spatial Patterns of Relatedness: Evidence for Isolation by Distance	24
Population Structure and the Role of IBD	25
Factors Affecting Gene Flow	27
Management Implications.....	31
REFERENCES	33
SUPPLEMENTAL INFORMATION.....	S1

LIST OF TABLES

Table 1. $\Delta AICc$ values for single-predictor and multiple-predictor landscape resistance models across four genetic distance metrics (PCA10, PCA64, Fij, and Dps).....	22
--	----

LIST OF FIGURES

Figure 1. Map showing the transect lines of aerial surveys that took place during winter 2024. Surveys were performed at 3 km intervals to identify caribou cratering sites for fecal sampling. Ground crews then accessed the cratering sites to collect samples, indicated by the black dots. The gray area represents the Churchill Caribou Range.....	8
Figure 2. Mantel correlograms showing Mantel correlation (r) against geographic distance in kilometers (km). Significant values are denoted by black dots.	18
Figure 3. Spatial genetic cluster assignments for woodland caribou. (A) STRUCTURE results at $K = 3$, showing individual cluster membership proportions by sampling location. (B) GENELAND posterior mode assignment map indicating five spatial clusters ($K = 5$) across the study area. (C) BAPS estimated a single ($K = 1$) cluster.	20
Figure 4. Maps showing the top supported model for each of the four genetic distances. The single-predictor model for wetlands is represented for PCA10, PCA64, and Dps, while the multiple-predictor conifer + water model is shown for Fij. Yellow/green indicates high resistance, while dark blue indicates low resistance.	23

LIST OF SUPPLEMENTAL MATERIALS

Supplemental Table S1. Primer information, including loci names, size range, primer concentration (μM), 5' dye, forward and reverse primer sequences.

Supplemental Table S2. Summary of multiple-predictor resistance surface models evaluated in step 2 of model selection. Each model tests a specific hypothesis about how landscape features may facilitate or impede gene flow in woodland caribou.

Supplemental Table S3. Summary of microsatellite diversity statistics for each genetic neighbourhood.

Supplemental Table S4. Summary of single-predictor resistance surface model performance for each of four genetic distance metrics. For each surface, only the top-performing replicate is reported.

Supplemental Figure S1. Raster layer showing the proportion of conifer cover within a 1000 m moving window across the Churchill Range. Values range from 0 (absence) to 1 (complete cover). Red points indicate sampled caribou locations.

Supplemental Figure S2. Raster layer showing the proportion of deciduous cover within a 1000 m moving window across the Churchill Range. Values range from 0 (absence) to 1 (complete cover). Red points indicate sampled caribou locations.

Supplemental Figure S3. Raster layer showing the network of roads across the range within a 1000 m moving window across the Churchill Range. Values range from 0 (absence) to 1 (complete cover). Red points indicate sampled caribou locations.

Supplemental Figure S4. Raster layer showing the proportion of fire cover within a 1000 m moving window across the Churchill Range. Values range from 0 (absence) to 1 (complete cover). Red points indicate sampled caribou locations.

Supplemental Figure S5. Raster layer showing the proportion of conifer cover within a 1000 m moving window across the Churchill Range. Values range from 0 (absence) to 1 (complete cover). Red points indicate sampled caribou locations.

Supplemental Figure S6. Raster layer showing the proportion of waterbody cover within a 1000 m moving window across the Churchill Range. Values range from 0 (absence) to 1 (complete cover). Red points indicate sampled caribou locations.

Supplemental Figure S7. Raster layer showing the proportion of wetland cover within a 1000 m moving window across the Churchill Range. Values range from 0 (absence) to 1 (complete cover). Red points indicate sampled caribou locations.

Supplemental Figure S8. Summary statistics for STRUCTURE runs across different values of K used to determine the most likely number of genetic clusters. (A) Mean $[\ln P(K)] \pm \text{SD}$ across replicate runs for each K . (B) First-order rate of change in $\ln P(K)$ with respect to K . (C) Second-order rate of change in $\ln P(K)$, or $L''(K) \pm \text{SD}$, used in the calculation of ΔK . (D) ΔK values, which reflect the rate of change in the log likelihood between successive K values. SD = standard deviation.

Supplemental Figure S9. STRUCTURE bar plot showing individual genetic assignment probabilities for $K = 3$ genetic clusters. Each bar represents one individual, with color proportions indicating the estimated fraction of that individual's genome assigned to each cluster.

INTRODUCTION

Preserving ecological integrity to support biodiversity has become increasingly important as landscapes face rising pressures from human development and climate change (Bellard et al. 2012, Keck et al. 2025). A key concern for species at risk is the disruption of gene flow, which maintains genetic diversity, reduces inbreeding, and supports adaptive capacity (Manel and Holderegger 2013, Sexton et al. 2024). Habitat fragmentation caused by natural and anthropogenic disturbances can significantly alter population structure and reduce genetic connectivity (Keyghobadi 2007, Rivera-Ortíz et al. 2015). Fragmented landscapes limit dispersal opportunities, leading to genetic isolation and increased genetic differentiation among subpopulations (Frankham et al. 2010). Isolated populations face elevated extinction risk due to reduced genetic diversity, demographic instability, and a diminished likelihood of rescue via immigration. Understanding how various landscape features influence genetic connectivity is therefore central to effective conservation planning (Manel et al. 2003, Sork and Waits 2010).

Landscape genetics provides a framework for quantifying how gene flow is shaped by both geographic distance and environmental heterogeneity (Manel et al. 2003). One of the most common patterns observed is isolation by distance (IBD), where genetic differentiation increases with geographic separation due to spatial limits on dispersal (Wright 1943). In highly mobile species, this relationship is often weaker than in more sedentary species because individuals can travel long distances and maintain gene flow across broader areas (Hillman et al. 2014). Still, even in mobile species, landscape configuration can influence movement behavior in ways that may not be evident from geographic distance alone (Coulon et al. 2004; Palm et al. 2023)

To address this, landscape genetics increasingly examines isolation by resistance (IBR), a framework that links genetic connectivity to the permeability of the landscape. IBR occurs when specific environmental features reduce or enhance the probability of successful dispersal, regardless of straight-line distance (McRae 2006). For example, roads, logged areas, or water bodies may act as resistance features (Courtois et al. 2008, Fortin et al. 2008, Anderson and Thomson 2024), while features such as continuous forest or wetlands are generally associated with increased connectivity (Stuart-Smith et al. 1997, Hornseth and Rempel 2016). The strength and direction of resistance effects can vary depending on spatial scale, species ecology, and landscape context (Palm et al. 2023). Distinguishing IBD from IBR is critical for understanding the ecological processes shaping genetic structure, especially in conservation settings where targeted habitat protection or restoration is needed to support connectivity (Manel et al. 2003).

Woodland caribou (*Rangifer tarandus caribou*) are listed as threatened under the Canadian Species at Risk Act (SARA) and the Ontario Endangered Species Act (ESA). Boreal populations face ongoing declines (Environment Canada 2012, Lelotte et al. 2025) and reduced genetic diversity has been observed in some regions, particularly in southern parts of the range where landscape disturbance and range retraction are most pronounced (Thompson et al. 2019). These patterns raise concerns about long-term population viability, especially where gene flow is limited and local extirpation risk is high.

Relatively few landscape genetic studies have explicitly evaluated which features impede gene flow in boreal caribou (Weckworth et al. 2013, Priadka et al. 2019, Anderson and Thomson 2024). Among those that have, roads and waterbodies have emerged as potential contributors to genetic differentiation (Priadka et al. 2019, Anderson and Thomson 2024). Across boreal regions

of Alberta, Saskatchewan, and Manitoba, (Priadka et al. 2019) found that isolation by distance (IBD) was the dominant pattern, but resistance models incorporating roads consistently explained spatial genetic structure, with waterbodies contributing in eastern regions. Fire, by contrast, was the least important variable and did not improve model fit relative to IBD. In Ontario, a ResistanceGA-based analysis by Anderson and Thomson 2024 similarly identified roads as the only consistent predictor of genetic structure, with fire offering no better explanatory power than IBD. In contrast, Weckworth et al. 2013 found that resistance models including disturbance and landscape features did not explain genetic structure better than IBD alone in Alberta populations. These mixed findings may reflect regional differences in landscape context or variation in study design and scale. Notably, none of these studies evaluated whether natural features might facilitate gene flow - a critical omission given the potential for intact habitat, wetlands, or other low-resistance elements to promote connectivity.

Several approaches have been used to evaluate the influence of landscape features on gene flow. Exploratory methods such as MEMGENE (Galpern et al. 2014) partition spatial genetic variation using Moran's eigenvector maps, offering insights into broad- and fine-scale spatial structure. However, MEMGENE does not directly test landscape hypotheses, and landscape interpretations must be conducted post hoc using resistance surfaces that are often subjectively defined. Similarly, basic regression approaches (e.g., partial Mantel tests or MLPE models), and circuit theory-based tools such as Circuitscape (McRae et al. 2008, Shah and McRae 2008) require researchers to assign resistance values a priori (e.g., Ruiz-Gonzalez et al. 2015, Emel et al. 2019). While Circuitscape is a powerful tool for modeling movement across heterogeneous landscapes, it cannot determine optimal resistance values without external input

and thus shares the same limitation of subjectivity. These methods often test only a narrow range of assumptions and may not adequately reflect the complexity of movement across real-world landscapes. In contrast, *ResistanceGA* (Peterman 2018) uses a genetic algorithm to iteratively search resistance parameter space and identify values that best explain observed genetic differentiation. Competing models are evaluated using AIC-based model selection, allowing researchers to empirically determine which landscape features and combinations provide the strongest fit. This optimization framework reduces bias, increases reproducibility, and enables a more realistic, data-driven assessment of functional connectivity.

While resistance-based models have been used to explore caribou connectivity, most emphasize impediments to movement such as roads, harvest blocks, and seismic lines, and rely on subjectively assigned resistance values or limited scenario testing (Weckworth et al. 2013, Priadka et al. 2019). Natural features that may facilitate gene flow, such as contiguous forest, wetlands, or intact habitat, are rarely incorporated despite their ecological importance and their roles in habitat selection and predator avoidance (Bergerud 1985, Rettie and Messier 2000, Courbin et al. 2009). This omission may lead to an incomplete or biased understanding of functional connectivity, particularly for a wide-ranging species like boreal caribou, whose movement is shaped by both avoidance of risk and attraction to safe or resource-rich environments (Rettie and Messier 2000, Mumma et al. 2019). Recognizing these dual influences is critical for developing conservation strategies aimed at maintaining gene flow and demographic connectivity across fragmented ranges. By explicitly evaluating potential facilitators of movement alongside traditional resistance features, our study addresses this gap

and contributes to a more balanced and ecologically grounded understanding of landscape connectivity in caribou.

The objectives of this study are to (1) provide the first comprehensive, fine-scale assessment of population genetic structure in the Churchill Range, establishing a baseline for conservation and land-use planning, and (2) identify which landscape features most strongly facilitate or impede genetic connectivity in woodland caribou. We hypothesize that natural features such as wetlands and contiguous forest act as key facilitators of gene flow, while anthropogenic features such as roads and harvest areas act as barriers. We further hypothesize that models incorporating multiple features-both facilitators and resistors-offer a more realistic explanation of genetic structure than models based on any single factor. By clarifying the landscape factors that shape connectivity in the Churchill Range, this study provides conservation practitioners with evidence-based guidance for protecting key habitats and mitigating barriers. The results establish a genetic baseline for woodland caribou in this range and contribute directly to landscape-level planning to support their long-term persistence.

METHODS

Study Area

The Churchill Range is located north of Sioux Lookout, Ontario, and forms part of the continuous distribution of woodland caribou in the province. Covering an area of 21,300 km², the range is primarily forested, with extensive wetlands and numerous lakes. Prominent waterbodies within the range include De Lesseps Lake, Churchill Lake, Birch Lake, Confederation Lake, Lac Seul, and Lake St. Joseph - all of which are considered important calving lakes (MNR 2014). The Cat River lake-chain forms the northern boundary of the range.

Geologically, the Churchill Range lies within the Boreal Shield, underlain by Precambrian bedrock and shaped by glacial features such as eskers, moraines, and sandy outwash deposits (MNR 2014). The soils are generally non-calcareous and poorly developed, with areas of exposed bedrock, thin soil cover, and extensive wetlands. These include treed bogs and fens dominated by black spruce (*Picea mariana*), sedges, and mosses. Peatlands are widespread, supporting carbon storage, poor drainage, and seasonal caribou refuge habitat. Coniferous forests throughout the range also provide critical winter forage in the form of arboreal and terrestrial lichens (*Cladonia* spp.).

Climate data from 1991 to 2020 for Sioux Lookout indicate an average annual precipitation of 776.7 mm, with 209.5 mm falling as snow (Environment Canada 2020). The average daily temperature over the same period was 2.1 °C. These cool, moist conditions support the persistence of boreal ecosystems.

Disturbances in the Churchill Range have been shaped by both natural events and human activity (MNRF 2014). Historical fires have had a major influence, with significant burns occurring in 1940, 1961, 1996, 2003, and 2011. The 2012 Integrated Range Assessment found that 41.3% of the range had been disturbed, with 35.9% attributed to anthropogenic sources (e.g., harvest blocks, roads, hydro lines) and 5.4% to natural causes (MNRF 2014). Roads are concentrated in the southern and central portions of the range near Sioux Lookout, ON, with density decreasing toward the north (Supplemental Figure S5). Waterbodies accounted for an additional 20.1% of the range area.

A minimum animal count (MAC) from the 2012 Integrated Range Assessment (MNRF 2014) estimated 262 caribou within the range, with the short-term population trend indicating stability or a slight decline ($\lambda = 0.96$). Caribou in the Churchill Range occur in small, dispersed groups and show strong fidelity to seasonal habitats, particularly calving sites.

Sample Collection

Between January and March 2024, fecal samples were collected during aerial surveys flown at 3 km transect intervals, with sampling conducted at the beginning of each month. Caribou signs such as tracks or cratering sites were identified from fixed-wing aircraft, and ground crews accessed collection sites via helicopter. At each site, field crews aimed to collect approximately 1.4 times the estimated number of animals using the area, based on visual estimates of cratering intensity, track counts, and pellet group distribution. This strategy was designed to reduce the likelihood of missing any individuals present, while minimizing oversampling of the same individual. Pellets were collected only from clearly separated, discrete pellet groups. Each sample was handled using sterile, single-use tools and placed into a uniquely

labeled bag. Efforts were made to ensure that each bag contained fecal material from a single defecation event to reduce the risk of collecting mixed samples from multiple individuals. The geographic coordinates of each collection site were recorded using handheld GPS units (± 5 m accuracy) and later used to extract spatial environmental data and link individual genotypes to landscape variables in subsequent analyses. Samples were kept on ice in the field and transferred before being transferred to a -20°C freezer for long term storage. In total, 600 samples were collected across 34 sites during the 2024 survey period (Figure 1).

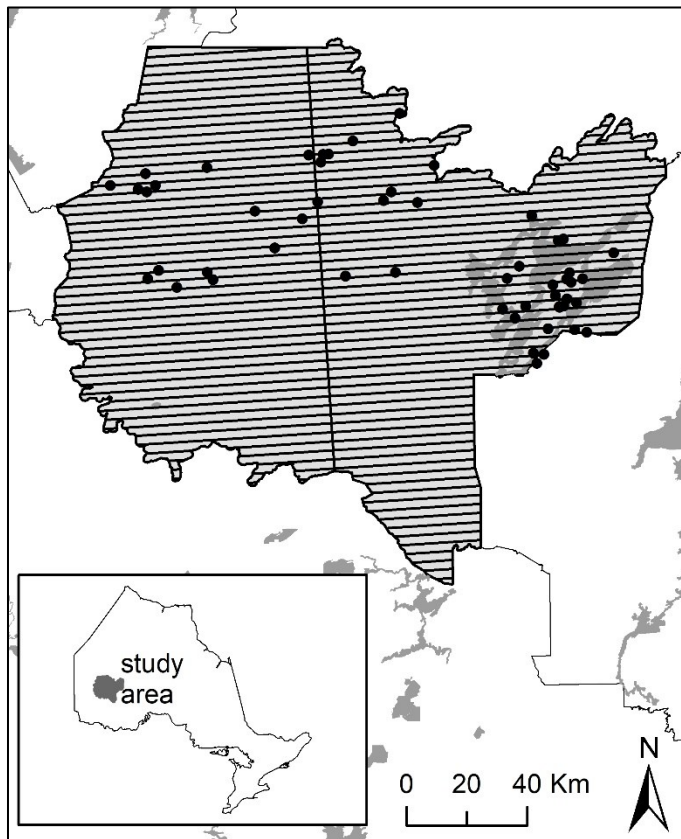


Figure 1. Map showing the transect lines of aerial surveys that took place during winter 2024. Surveys were performed at 3 km intervals to identify caribou cratering sites for fecal sampling. Ground crews then accessed the cratering sites to collect samples, indicated by the black dots. The gray area represents the Churchill Caribou Range.

DNA Extraction and Genotyping

DNA was extracted from four pellets per fecal sample using the Qiagen DNeasy Blood and Tissue Kit, following a modified protocol based on Ball et al. (2007). DNA concentration was then quantified with a Nanodrop One spectrophotometer (Thermo Fisher Scientific 2023), and extracts were standardized to approximately 20 ng/μL for downstream analyses.

Each sample was genotyped at 13 microsatellite loci using three multiplex PCR reactions (see Supplementary Table S1 for details). Amplified products were submitted to the Centre for Applied Genomics (Toronto, ON) for fragment size analysis on a SeqStudio™ Flex Genetic Analyzer (Applied Biosystems, Thermo Fisher Scientific, USA). Allele peaks were scored in GeneMarker® v3.0.1 (SoftGenetics LLC, State College, PA, USA). following standardized scoring guidelines. Each locus was independently scored by three individuals, and consensus genotypes were generated through comparison of scores to ensure consistency and reduce subjectivity. To ensure genotype accuracy, we reamplified and rescored any samples that had ambiguous peaks, no clear genotype matches, or matched other samples with only one or two allele mismatches indicating potential genotyping errors. Genotyping error rates were quantified by fully replicating a 96-well plate of randomly selected samples across all three multiplexes. Any discrepancies between replicate and original genotypes, excluding cases of missing data, were classified as genotyping errors and used to calculate an overall error rate.

Genetic Data Filtering and Quality Control

To avoid bias from duplicate genotypes, we used the *allelematch* R package (Galpern et al. 2012a) to identify individuals with identical multilocus genotypes. For each duplicated genotype, one occurrence was retained at random for downstream analyses. Marker performance

was evaluated by testing for deviations from Hardy-Weinberg Equilibrium (HWE) using exact test implemented in the R package *pegas* (Paradis 2010). HWE was assessed both globally and within populations, where populations were defined according to sampling period (i.e., January, February, or March). To assess non-random association among loci, we calculated the standardized index of association (\bar{r}_d) using the *poppr* R package (Kamvar et al. 2014) which accounts for multilocus linkage disequilibrium. We also estimated the frequency of null alleles for each locus using *poppr*, as excessive null allele frequencies can indicate unreliable markers.

Genetic Distance and Spatial Autocorrelation

We calculated four individual-level genetic distance metrics to characterize spatial genetic structure. First, we calculated pairwise kinship coefficients (F_{ij}) using the formulation of (Kalisz et al. 2001), implemented in the *gstudio* package (Dyer 2014). The proportion of shared alleles (Dps) was calculated using the `propShared()` function from the *adegenet* package (Jombart 2008). For multiple-predictor genetic distances, we constructed a table of allele counts for each individual, centered and scaled the data, and then conducted principal component analysis (PCA) using the `dudi.pca()` function in *adegenet*. We retained the first 10 and 64 principal components to capture broad- and fine-scale structure, respectively, following the recommendations of Shirk et al. (2017) and Beninde et al. (2024). Euclidean distances among individuals were then calculated from the PCA coordinates using the `distance()` function in the *ecodist* R package v2.1.3 (Goslee and Urban 2007) resulting in two distance matrices: PCA10 and PCA64.

To assess potential isolation by distance, we performed Mantel correlogram analyses using the `mgram()` function from the *ecodist* R package (Goslee and Urban 2007) with all

matrices converted to dissimilarity form. Geographic distance calculated as pairwise Euclidean distances from UTM coordinates (EPSG:26915), using the base R `dist()` function. To avoid exact spatial duplicates, coordinates were jittered by up to 100 m. Correlograms were generated using 1,000 permutations to test significance, and 500 bootstraps to estimate 90% and 95% confidence intervals. We applied fixed bin widths and a one-sided test to detect positive spatial autocorrelation. The spatial scale of positive genetic structure was defined as the midpoint of the largest distance class showing consistent positive Mantel correlation across all genetic distance metrics. This value was used as the genetic neighbourhood size (radius) in downstream diversity calculations.

Genetic Diversity and Relatedness

We quantified fine-scale patterns of genetic diversity using the *sGD* R package (Shirk and Cushman 2011), which calculates spatially explicit diversity metrics for individual-centered neighbourhoods. Neighbourhoods were defined using a 15 km radius based on results from spatial genetic structure analyses, with a minimum size of 10 individuals to ensure robust estimates. We used `summary_stats()` to calculate five standard metrics within each neighbourhood: observed heterozygosity (H_o), inbreeding coefficient (F_{IS}), allelic richness (A_r), private alleles (A_p), and total allele count (A). To avoid pseudoreplication due to multiple overlapping neighbourhoods within the same sampling site, we filtered the *sGD* output to retain a single representative neighbourhood per site. Specifically, we selected the neighbourhood with the largest number of individuals to ensure robust and non-redundant estimates.

Population Structure

To quantify population differentiation, pairwise Weir and Cockerham's F_{ST} values (Weir and Cockerham 1984) were calculated among genetic neighbourhoods using the `genet.dist()` function with the 'WC84' method in the *hierfstat* package (Goudet 2005). Population structure was first assessed using STRUCTURE v2.3.4 (Pritchard et al. 2000), applying the admixture model with correlated allele frequencies to account for potential gene flow among populations. Analyses were conducted for $K = 1$ to 10, with five replicates per K , each consisting of 100,000 burn-in iterations followed by 100,000 MCMC iterations. Log-likelihood values were summarized, and ΔK was calculated using the `evannoMethodStructure()` function in the *pophelper* R package v2.3.1 (Francis 2017) following the method of Evanno et al. (2005) to infer the most likely number of genetic clusters. Replicate runs for $K = 3$ were aligned using `alignK()` and visualized as Q-plots using `plotQ()`, with custom color schemes to represent cluster membership. To examine spatial trends in admixture, mean cluster assignment values were summarized by collection site and visualized as pie charts using *scatterpie* v0.2.5 (Yu 2016), positioned according to the UTM coordinate of each sampling site.

Population genetic structure was also evaluated using BAPS v6.0 (Corander et al. 2008) a Bayesian clustering method that incorporates spatial information as priors on cluster membership (François and Durand 2010). The "spatial clustering of individuals" option was applied for the population mixture analysis. Values of K from 1 to 10 were tested, with 10 replicates per K . Admixture analysis was then performed using the results of the mixture analysis, with the following settings: a minimum of five individuals per cluster, 50,000 MCMC iterations, 50 reference individuals per cluster, and 1,000 iterations for estimating admixture proportions.

Finally, we used the *Geneland* package v4.9.2 (Guillot et al. 2009) in R to identify spatial patterns of genetic structure while accounting for coordinate uncertainty. The spatial model with correlated allele frequencies (`freq.model = "Correlated"`) was applied, allowing the number of populations to vary from 1 to 10 (`varnpop = TRUE`, `npopmax = 10`). Coordinate uncertainty was set to 7 km (`delta.coord = 7`), reflecting the average winter home range diameter of woodland caribou in northwestern Ontario (Ferguson and Elkie 2004). Each MCMC chain was run for 100,000 iterations with thinning every 100 steps, and five independent chains were executed. Post-processing used a burn-in of 200 steps and included visualization of the posterior distribution of K (`Plotnpop`) and spatial assignment maps (`PosteriorMode`). The most likely number of populations was inferred by comparing mean posterior densities across runs. Individual assignments from *Geneland* and BAPS were converted to spatial features and overlaid on the Churchill range boundary and plotted using *ggplot2* (Wickham 2016) with cluster identities represented by color.

Landscape Variables

To evaluate spatial variation in landscape resistance to caribou movement, we compiled a suite of habitat and disturbance covariates informed by previous studies on woodland caribou habitat selection and distribution. These included forest composition (Wittmer et al. 2007, Courbin et al. 2009, Hornseth and Rempel 2016), linear features such as roads (Fortin et al. 2008; Galpern et al. 2012; Beauchesne et al. 2013) forest fire (Joly et al. 2003, Konkolics et al. 2021), forest harvest (Vors et al. 2007, Courtois et al. 2008, Fryxell et al. 2020), water (Ferguson and Elkie 2005, Hornseth and Rempel 2016), and wetlands (Hornseth and Rempel 2016). All spatial data were obtained from the Ontario GeoHub (Ontario 2024), the Ontario Ministry of

Natural Resources and Forestry, and Sustainable Forest License (SFL) holders (Orchard et al., in preparation). Spatial layers were projected in NAD83 / Ontario MNR Lambert (EPSG:3161).

Land cover data were derived from the Ontario Land Cover Composition Classification v2 (OLCCv2), which was reclassified into binary rasters indicating the presence (1) or absence (0) of four cover types: coniferous, deciduous, wetland, and water. Binary rasters were also created to represent recent fire (≤ 40 years) and recent harvest (≤ 35 years), with the latter buffered by 500 m to account for edge effects (Environment Canada 2012). Roads were represented as a binary raster of linear features. All rasters were initially processed at 15×15 m resolution. To summarize landscape context at a biologically relevant scale, each binary raster was aggregated to 1×1 km resolution using the `aggregate()` function in the *terra* R package (Hijmans 2020) summing the number of presence cells within each grid cell. This process yielded continuous rasters representing local density or coverage of each feature, which were exported in ASCII format for resistance surface modeling. Maps of the seven resistance surfaces (conifer, deciduous, roads, fire, harvest, water, and wetlands) are provided in the supplementary materials (Supplemental Figures S1-S7).

Resistance Surface Modeling

We used a two-step framework to evaluate how landscape features influence gene flow in woodland caribou. In the first step, we conducted an exploratory analysis by fitting single-predictor resistance surfaces for each landscape variable using the *ResistanceGA* R package (Peterman 2018). Variables included conifer, deciduous, wetlands, water, fire, roads, and harvest. In the second step, we constructed a targeted set of multiple-predictor models to test specific

hypotheses about the relative influence of landscape features that may facilitate versus impede gene flow (Supplemental Table S2).

For single surface models, individual resistance surfaces were optimized using the `SS_optim()` function in *ResistanceGA* (Peterman 2018) , incorporating genetic distance matrices and spatial coordinates as input through the `gdist.prep()` function. Multiple-predictor models were constructed by first standardizing all raster layers to a common extent with the `crop()` and `intersect()` functions. Aligned rasters were then stacked and optimized using the `MS_optim()` function. All models employed cost-distance genetic algorithms with a log-likelihood (LL) optimization framework and a maximum parameter value of 250 for continuous surfaces. Each resistance surface was evaluated using a mixed-effects model with a maximum-likelihood population effects (MLPE) structure, and model performance was compared using corrected Akaike Information Criterion (AIC_C). ResistanceGA optimizations were conducted on the Graham high-performance computing cluster through the Digital Research Alliance of Canada to reduce processing time.

RESULTS

Marker Quality Assessment

Of the 600 samples originally genotyped, a total of 11 were excluded from all analyses. Nine were removed due to sample handling issues or poor genotype quality (e.g., multiple peaks), one was removed due to excessive missing data, and one was excluded based on quality control inconsistencies identified during scoring. *Allelematch* analysis was then conducted on the remaining 589 samples, identifying 244 unique multilocus genotypes. Genotyping error rates ranged from 0 – 3.2%, with an average of 0.98 across loci. Three loci (FCB193, RT24, RT27) deviated from HWE globally, but no locus failed HWE in more than one population. For example, RT24 showed a significant global deviation but conformed to HWE in two of the three populations. Linkage disequilibrium across loci was low: the highest observed r^2 value (between RT5 and RT30) was approximately 0.06. The average estimated frequency of null alleles across all loci was 0.04, ranging from <0.01 to 0.11, well below the recommended exclusion threshold of 0.20 (Chapuis and Estoup 2007). Given that that no loci deviated from HWE across populations, null allele frequencies were low, and linkage disequilibrium was minimal, all 13 loci were retained to maximize analytical power.

Genetic Structure and Diversity

Mantel correlograms revealed significant positive spatial autocorrelation in genetic distance at short geographic distances for all genetic distance metrics examined (Figure 2). All four metrics showed positive autocorrelation in the first two lag classes (0–10 km and 10–20 km). However, only the first lag class (0–10 km) was significant ($p \leq 0.001$) across all metrics. Based on the largest lag class where all metrics showed positive autocorrelation, we

selected 15 km, the midpoint of the 10–20 km class, as the radius for defining genetic neighbourhoods.

Across the 46 genetic neighbourhoods, observed heterozygosity (H_o) ranged from 0.61 to 0.75, with a mean of 0.68, while expected heterozygosity (H_s) ranged from 0.63 to 0.72 (mean = 0.69) (Supplemental Table S3). Allelic richness (A_r), rarefied to a standardized neighbourhood size of 10 individuals, varied from 4.75 to 5.63, with a mean of 5.19 alleles per locus, and raw allele counts (A) ranged from 5.2 to 7.8 per locus (mean = 6.7). Inbreeding coefficients (F_{IS}) were generally low (mean = 0.0098), ranging from -0.117 to 0.082 , with most neighbourhoods showing near-zero or slightly positive values. Neighbourhood sample sizes ranged from 10 to 58 individuals, with an average of 31.4.

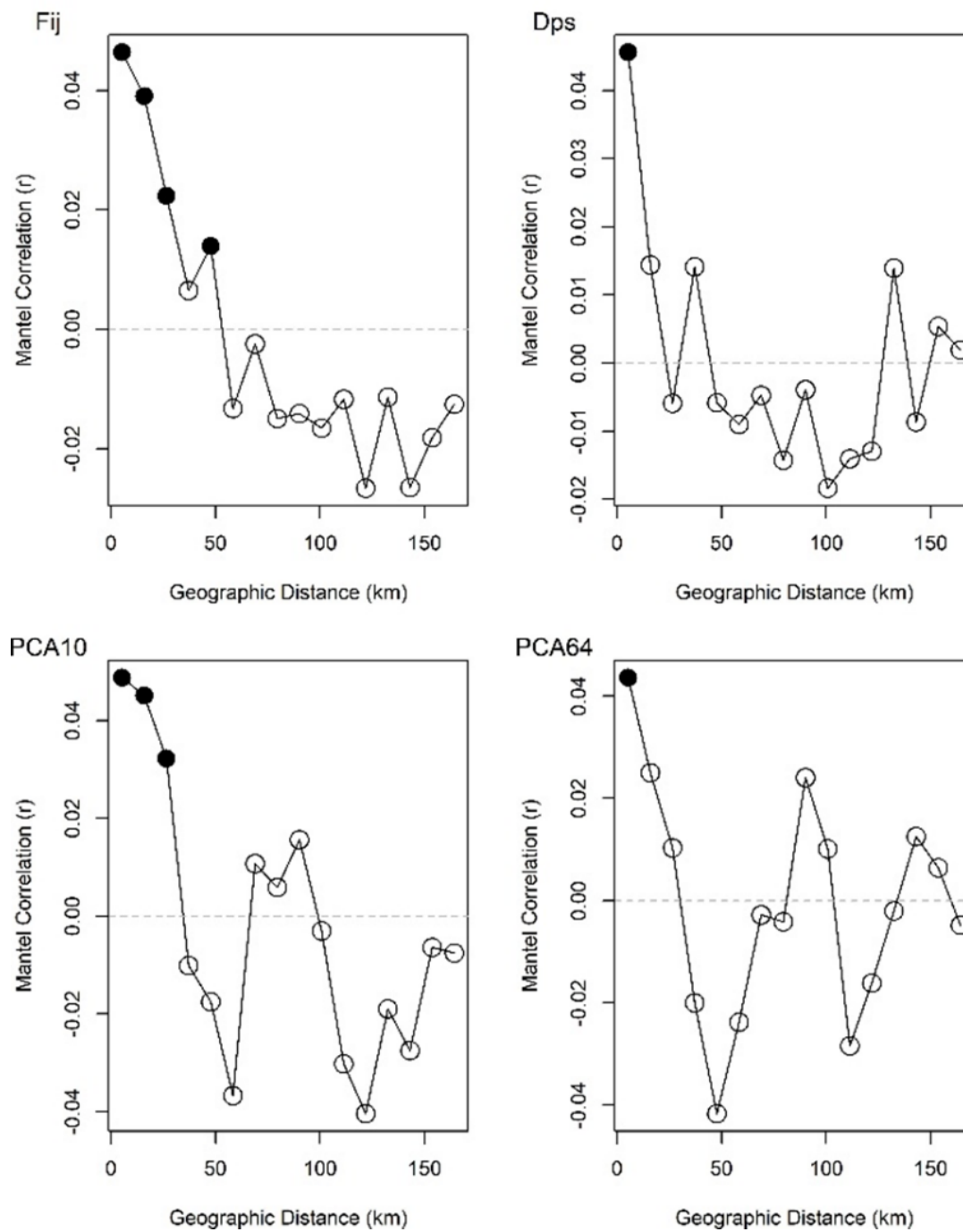


Figure 2. Mantel correlograms showing Mantel correlation (r) against geographic distance in kilometers (km). Significant values are denoted by black dots.

Pairwise F_{ST} values among neighbourhoods were extremely low (< 0.003), indicating that over 99.7% of genetic variation occurs within, rather than between, neighbourhoods. Mantel correlation coefficients were also low ($r \leq 0.04$), reflecting weak spatial genetic structure. Genetic clustering analyses produced contrasting results across methods. STRUCTURE identified $K = 3$ as the most likely number of genetic clusters based on the Evanno method clusters (Supplemental Figure S8). In contrast, BAPS supported $K = 1$, while GENELAND inferred $K = 5$ spatial clusters across the study area. Visual inspection of STRUCTURE and GENELAND assignment plots revealed broad geographic structuring with possible isolation along the eastern range boundary.

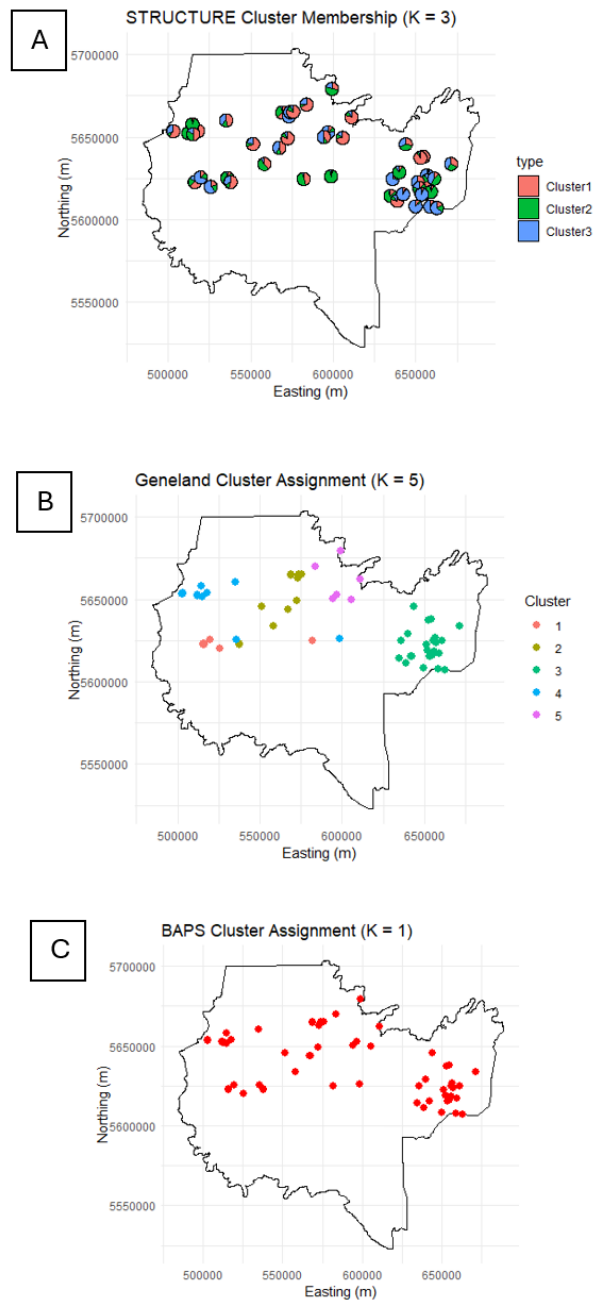


Figure 3. Spatial genetic cluster assignments for woodland caribou. (A) STRUCTURE results at $K = 3$, showing individual cluster membership proportions by sampling location. (B) GENELAND posterior mode assignment map indicating five spatial clusters ($K = 5$) across the study area. (C) BAPS estimated a single ($K = 1$) cluster.

Factors Affecting Gene Flow

Single-predictor resistance models revealed that the top-performing surface differed by genetic distance metric. Wetlands was the top single-predictor model for Dps, PCA10, and PCA64 (R^2_m ranging from 0.001 to 0.009), and was consistently fit with an inverse monomolecular transformation, indicating declining resistance with increasing percent wetland cover (Supplemental Table S4). For Fij, the top-ranked single-predictor resistance model was conifer ($R^2_m = 0.006$), followed by roads, harvest, fire, geographic distance, and deciduous, all within $\Delta AICc < 15$.

Multiple-predictor model comparisons revealed that combining wetlands with other surfaces did not improve model performance for Dps, PCA10, or PCA64. In all three cases, the single-predictor wetlands model outperformed the top multiple-predictor alternatives, including combinations with conifer, roads, water, harvest, or fire (Table 1). For example, the addition of conifer to wetlands increased $\Delta AICc$ values by 6.7 (PCA10), 7.2 (PCA64), and 10.0 (Dps). Only for Fij did a multiple-predictor model (conifer + water, $R^2_m = 0.001$) appear as the top model and outperform the single-predictor wetlands model.

Table 1. $\Delta AICc$ values for single-predictor and multiple-predictor landscape resistance models across four genetic distance metrics (PCA10, PCA64, Fij, and Dps).

Model	Dps $\Delta AICc$	PCA10 $\Delta AICc$	PCA64 $\Delta AICc$	Fij $\Delta AICc$
Wetlands only†	0.0	0.0	0.0	15.5
Conifer only†	13.9	37.5	20.9	4.5
Wetlands + Conifer	10.0	6.7	7.2	3.3
Wetlands + Roads	9.5	11.1	9.5	13.5
Wetlands + Water	8.8	13.1	6.3	19.0
Wetlands + Harvest	8.4	13.6	7.7	16.1
Wetlands + Fire	9.5	9.8	2.9	19.0
Roads + Harvest	7.5	31.2	17.8	12.6
Wetlands + Roads + Conifer	8.7	10.9	12.2	9.2
Conifer + Water	-	-	-	0.0
Conifer + Fire	-	-	-	8.9
Conifer + Deciduous	-	-	-	9.0
Conifer + Harvest	-	-	-	10.5
Conifer + Roads	-	-	-	12.0

† Single-predictor baseline models.

Bold indicates the best model ($\Delta AICc = 0$) for each metric.

- Indicates model that wasn't run for a particular distance metric

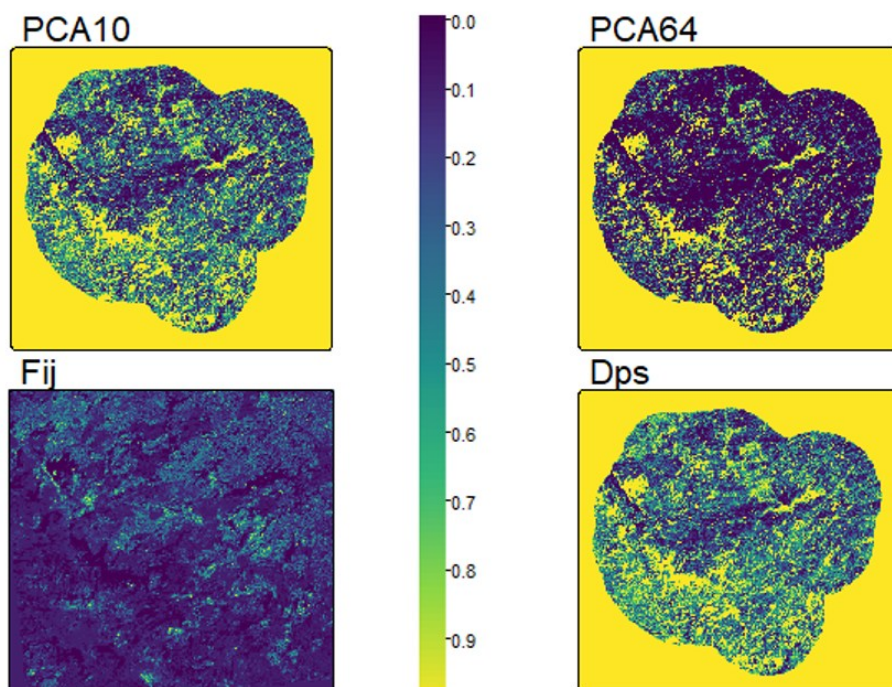


Figure 4. Maps showing the top supported model for each of the four genetic distances. The single-predictor model for wetlands is represented for PCA10, PCA64, and Dps, while the multiple-predictor conifer + water model is shown for Fij. Yellow/green indicates high resistance, while dark blue indicates low resistance.

DISCUSSION

Overview of Genetic Connectivity and Diversity

Our findings indicate that woodland caribou in the Churchill Range exhibit moderate genetic diversity and weak population structure, suggesting a relatively cohesive population. Expected heterozygosity ($H_e = 0.68$) aligns closely with values reported in other boreal caribou populations in central and northern Canada (e.g., Thompson et al. 2019, Fournier 2024) and remains considerably higher than in severely isolated herds such as Atlantic-Gaspésie (Yannic et al. 2016). This level of diversity implies that Churchill caribou retain meaningful adaptive potential under current conditions.

Inbreeding coefficients (FIS) were low or slightly negative across most neighbourhoods, with a mean of 0.01. This suggests a low likelihood of inbreeding. Slightly positive values may reflect mild Wahlund effects due to overlapping kin groups, or technical artifacts associated with null alleles at a few loci (De Meeûs 2018).

Spatial Patterns of Relatedness: Evidence for Isolation by Distance

Spatial autocorrelation analyses revealed significant positive genetic correlation at short distances (0–10 km), with weaker but still positive correlations observed in the 10–20 km range. This pattern is consistent with isolation by distance (IBD), in which geographically proximate individuals are more genetically similar due to spatial limits on dispersal. Dispersal distances reported by (McFarlane et al. 2022) support this interpretation: average dispersal between parents and offspring was 20 km for females and 22 km for males, with the majority of events under 40 km. In addition, studies have shown strong site fidelity in woodland caribou, even in disturbed environments (Tracz et al. 2010), suggesting that overlapping home ranges and short-

distance natal dispersal can create fine-scale spatial genetic structure. These observations support a stepping-stone model of gene flow, in which gradual dispersal among neighboring individuals maintains connectivity across the landscape. Although we observed a decline in genetic similarity with distance, including some negative autocorrelation at longer distances, this pattern did not align with the presence of strong, discrete barriers. Instead, it likely reflects stochastic processes or reduced kinship among more distant individuals (Weckworth et al. 2013, Priadka et al. 2019). Although Mantel correlations were low ($r \sim 0.04$), this pattern is consistent with isolation by distance in wide-ranging species like woodland caribou, where weak but detectable genetic structure often emerges despite high dispersal capacity (Yannic et al. 2016). The small effect size likely reflects both the inherent noise of individual-based genetic distance measures and the expectation that most genetic variation is maintained within, rather than between, local groups (Shirk and Cushman 2011, Priadka et al. 2019). Thus, rather than indicating biological irrelevance, these results support the interpretation that caribou in the Churchill Range remain broadly connected, with gene flow occurring at fine spatial scales in the absence of strong barriers.

Population Structure and the Role of IBD

Model-based clustering algorithms produced inconsistent results regarding the number of genetic clusters (K). STRUCTURE supported $K = 3$, while BAPS identified $K = 1$, and GENELAND suggested up to five spatial clusters. However, assignment probabilities from STRUCTURE revealed a gradual cline in genetic composition rather than discrete groupings, suggesting that the program was detecting continuous genetic variation consistent with IBD rather than true population substructure. This result is not unexpected given the extremely low

FST value observed for our data ($F_{ST} < 0.003$) and are consistent with the known limitations of clustering algorithms under IBD and weak genetic differentiation, where subtle allele frequency gradients can lead to overestimation of population structure (Guillot et al. 2009, Meirmans 2012). Such extremely weak genetic differentiation is expected for wide-ranging species like caribou (Priadka et al. 2019).

Similarly, the high number of clusters inferred by GENELAND likely reflects spatial autocorrelation in the genetic data rather than discrete population boundaries. As a spatially explicit model, GENELAND assumes Hardy-Weinberg and linkage equilibrium within clusters and can misinterpret gradual spatial changes in allele frequencies as hard boundaries between populations (Guillot et al. 2009). In our study, the use of individual-level spatial coordinates and a 7 km spatial uncertainty buffer (reflecting typical home range size) may have further contributed to this artifact by amplifying fine-scale genetic differences. Comparable findings have been reported in other studies where spatial autocorrelation and fine-scale sampling resulted in spurious clustering in continuous populations lacking true barriers to gene flow (e.g. (Frantz et al. 2009)

These results align with earlier research in other woodland caribou ranges across Canada, where weak or inconsistent genetic clustering was commonly reported (Priadka et al. 2019, Anderson and Thomson 2024). Studies have concluded that population structure in boreal caribou is best described as continuous due to IBD rather than fragmented by discrete boundaries (Ball et al. 2010; Weckworth et al. 2013; Priadka et al. 2019, Anderson and Thomson 2024). In this context, the apparent clustering observed in our analyses likely reflects subtle spatial gradients in genetic differentiation, shaped by high dispersal ability and the absence of complete

barriers to gene flow. While we detected a strong signal of IBD, landscape resistance analyses (discussed below) also revealed some constraints on connectivity that may contribute to these patterns.

Factors Affecting Gene Flow

Our results provide partial support for the study's hypotheses regarding the drivers of genetic connectivity in woodland caribou. First, as predicted, natural features associated with movement facilitation, particularly wetlands, were stronger predictors of gene flow than anthropogenic resistance features when evaluated in single-predictor models. The single-predictor wetlands surface consistently outperformed all other resistance models, including distance-only, across three of four genetic distance metrics (Dps, PCA10, and PCA64), suggesting that wetlands function as low-resistance corridors that facilitate long-distance movement and gene flow across the Churchill Range. These habitats are known to offer travel routes, predator refugia, and foraging opportunities, particularly in landscapes with low road density (Brown et al. 2000, Keim et al. 2021).

For the remaining metric (Fij), the top-ranked model was the conifer + water combination, again highlighting the importance of natural features. The apparent negative correlation between $1 - F_{ij}$ and conifer cover should not be interpreted as conifer impeding connectivity. F_{ij} quantifies pairwise genetic similarity based on shared ancestry, making it particularly responsive to the spatial distribution of close relatives (Hardy 2003). In caribou, strong female philopatry and the formation of localized family groups can generate spatial clustering of related individuals (McFarlane et al. 2022). Because $1 - F_{ij}$ decreases as kinship increases, the observed pattern likely reflects higher kinship in conifer-dominated areas, where

high-quality habitat reduces the need for offspring to disperse farther from natal sites. This interpretation is consistent with ecological theory and previous work suggesting that site fidelity in caribou is shaped by both food quality and predation risk (Wittmer et al. 2006)

Together, these findings suggest that wetlands and conifer both influence caribou genetic structure, but in different ways and at different scales. Wetlands consistently facilitated gene flow across multiple allele frequency–based metrics, reflecting their role as broad-scale movement corridors over many generations. In contrast, the effect of conifer was detected only with the kinship-based *F_{ij}* metric and likely reflects fine-scale structuring driven by strong site fidelity and reduced dispersal in high-quality habitat. The complementary strengths of kinship-based and allele frequency–based metrics highlight the layered nature of gene flow, shaped by both short-term behavioral processes and longer-term ecological dynamics.

Contrary to our second hypothesis, multiple-predictor models combining facilitating and resistive features did not universally outperform the top single-predictor models. For three of four genetic distance metrics, the lowest AICc values were obtained from single-predictor surfaces, including wetlands for *D_{ps}*, PCA10, and PCA64, indicating that these habitat types exert the strongest influence on gene flow in the Churchill Range. However, *F_{ij}* exhibited a contrasting pattern with the conifer + water model outperforming all other models. Across all genetic distances, several multiple-predictor models, particularly those combining wetlands with conifer, fire, or roads, had ΔAICc values < 10 and should be considered as moderately supported alternatives. These models suggest that while dominant features like wetlands account for most of the explained variation, additional landscape elements may contribute meaningfully to gene flow when considered in combination. This supports the idea that cumulative landscape

permeability, shaped by both facilitators and barriers, governs genetic connectivity in woodland caribou (McLoughlin et al. 2004, Galpern et al. 2012*b*).

Among the resistance features evaluated, roads appeared in several models with $\Delta AICc < 10$ but did not show strong support relative to the top models. Roads are relatively dense across the southern and central portions of the Churchill Range, tapering off only in the north, yet their influence on connectivity was weak compared to natural facilitators such as wetlands. This finding contrasts with studies in other regions that have demonstrated stronger road effects on woodland caribou (Priadka et al. 2019, Anderson and Thomson 2024). Importantly, those earlier studies considered only potential barriers, whereas the present analysis also incorporated potential facilitators such as wetlands and conifer. From a conservation perspective, the weak road effect observed here highlights the importance of considering both resistance and facilitation processes in landscape genetics analyses, since focusing exclusively on barriers may overemphasize their role relative to natural features that promote connectivity.

Harvest and fire, while not strongly supported in single-predictor models, also appeared in several multiple-predictor combinations, particularly with wetlands or conifer, implying that these features may contribute to cumulative resistance when overlapping otherwise permeable habitat. Both features were associated with lower connectivity, but their independent effects appear limited in this landscape, with $\Delta AICc$ values exceeding 15 for most metrics.

Waterbodies were not well supported as standalone predictors ($\Delta AICc > 10$ across all metrics), but appeared in several competitive multiple-predictor models, including the top-ranked model for Fij (conifer + water). The inclusion of water in this model suggests a context-dependent influence on gene flow, likely shaped by seasonal dynamics. In winter, frozen lakes

and rivers may facilitate movement by providing direct, low-resistance travel corridors periods (McLoughlin et al. 2004, Avgar et al. 2013, Leblond et al. 2016), whereas open water during summer can impede dispersal due to the energetic costs of crossing and limited incentives (Leblond et al. 2016). The inverse-reverse monomolecular transformation applied to water indicates that large, contiguous water bodies were associated with low resistance, consistent with ice-facilitated winter dispersal. However, water may also reflect shoreline-associated travel or shared habitat use. This finding contrasts with (Priadka et al. 2019a), who reported moderate resistance associated with water in boreal caribou populations in Manitoba and Saskatchewan. Overall, the role of water in shaping genetic connectivity appears to vary regionally and seasonally, emphasizing the importance of ecological context when interpreting landscape resistance patterns.

Although several studies have emphasized resistance from anthropogenic features such as roads (Priadka et al. 2019, Anderson and Thomson 2024) cross-study comparisons reveal important differences. In particular, the stronger support for barriers reported in earlier work may partly reflect narrower model scopes: Priadka et al. 2019, Anderson and Thomson 2024 did not include natural facilitators as candidate resistance surfaces in their analyses. By explicitly evaluating both facilitators and resistive features, our study provides a more balanced assessment of landscape connectivity and highlights the dominant role of natural habitat elements, particularly wetlands, in shaping caribou gene flow. These findings suggest that apparent resistance effects in previous studies may reflect model limitations as much as true ecological barriers, reinforcing the importance of holistic modeling frameworks.

Management Implications

Woodland caribou in the Churchill Range exhibit extremely weak population structure and moderate genetic diversity, suggesting that this population remains genetically cohesive and retains adaptive potential. At the same time, our spatial genetic structure analysis revealed a significant pattern of isolation by distance, indicating that connectivity declines gradually with geographic distance. Understanding which landscape features shape this gradual structure is essential for guiding conservation and land-use planning.

Our analysis identified wetlands as the strongest and most consistent predictor of genetic connectivity, with wetlands-only models outperforming all alternatives based on allele frequency-based metrics (Dps, PCA10, PCA64). This emphasizes the critical role of wetlands in sustaining broad-scale gene flow and highlights the need to prioritize the conservation of large, continuous wetland complexes in management and planning (Racey et al. 1999, Brown et al. 2000, Keim et al. 2021).

The kinship-based Fij metric identified conifer in combination with water as the top model. This suggests that conifer habitats may influence genetic structure through more recent demographic processes, such as the spatial clustering of related individuals, consistent with female philopatry and site fidelity (Wittmer et al. 2006, McFarlane et al. 2022). In contrast, allele frequency-based metrics integrate gene flow across multiple generations and consistently identified wetlands as the dominant facilitator of connectivity. These complementary findings indicate that wetlands are the primary driver of long-term, broad-scale connectivity in the Churchill Range, while conifer habitats may contribute to structuring genetic relationships over shorter temporal scales.

Other features, including roads, harvest areas, fire, and waterbodies, showed weak and inconsistent effects in this range. Nevertheless, their importance in other contexts has been well documented: roads increase predation risk and are avoided by caribou (Fortin et al. 2008, Beauchesne et al. 2013) and landscape genetic studies that focused only on barriers have often identified roads as strong predictors of differentiation (Priadka et al. 2019b, Anderson and Thomson 2024)). Fire and waterbodies have also been linked to resistance in other studies (McLoughlin et al. 2004, Galpern et al. 2012b). Further study will be needed to determine whether the patterns observed in the Churchill Range are broadly applicable across other ranges, or whether the relative influence of facilitators and resistors varies with landscape context.

Taken together, these findings underscore the importance of considering both facilitators and resistors when evaluating caribou connectivity. For the Churchill Range, wetlands are clearly the dominant driver of broad-scale gene flow, while conifer (particularly in association with water) appears to shape more recent genetic relationships. Effective landscape planning should therefore prioritize the conservation of wetland complexes while also recognizing the potential contributions of conifer habitats and the possible influence of disturbance features such as roads, fire, and waterbodies.

REFERENCES

- Anderson, N., and A. M. Thomson. 2024. Landscape genetic analysis of population structure and factors influencing gene flow in a southern peripheral population of boreal woodland caribou (*Rangifer tarandus caribou*). *Conservation Genetics* 25:1265–1281.
- Avgar, T., A. Mosser, G. S. Brown, and J. M. Fryxell. 2013. Environmental and individual drivers of animal movement patterns across a wide geographical gradient. A. Myserud, editor. *Journal of Animal Ecology* 82:96–106.
- Ball, M. C., L. Finnegan, M. Manseau, and P. Wilson. 2010. Integrating multiple analytical approaches to spatially delineate and characterize genetic population structure: an application to boreal caribou (*Rangifer tarandus caribou*) in central Canada. *Conservation Genetics* 11:2131–2143.
- Ball, M. C., R. Pither, M. Manseau, J. Clark, S. D. Petersen, S. Kingston, N. Morrill, and P. Wilson. 2007. Characterization of target nuclear DNA from faeces reduces technical issues associated with the assumptions of low-quality and quantity template. *Conservation Genetics* 8:577–586.
- Beauchesne, D., J. Ag. Jaeger, and M.-H. St-Laurent. 2013. Disentangling Woodland Caribou Movements in Response to Clearcuts and Roads across Temporal Scales. D. Russo, editor. *PLoS ONE* 8:e77514.
- Bellard, C., C. Bertelsmeier, P. Leadley, W. Thuiller, and F. Courchamp. 2012. Impacts of climate change on the future of biodiversity. *Ecology Letters* 15:365–377.
- Beninde, J., J. Wittische, and A. C. Frantz. 2024. Quantifying uncertainty in inferences of landscape genetic resistance due to choice of individual-based genetic distance metric. *Molecular Ecology Resources* 24:e13831.
- Bergerud, A. T. 1985. Antipredator strategies of caribou: dispersion along shorelines. *Canadian Journal of Zoology* 63:1324–1329.
- Bishop, M. D., S. M. Kappes, J. W. Keele, R. T. Stone, S. L. Sunden, G. A. Hawkins, S. S. Toldo, R. Fries, M. D. Grosz, and J. Yoo. 1994. A genetic linkage map for cattle. *Genetics* 136:619–639.
- Brown, K. G., C. Elliott, and F. Messier. 2000. Seasonal distribution and population parameters of woodland caribou in central Manitoba: implications for forestry practices. *Rangifer* 20:85.
- Buchanan, F. C., and A. M. Crawford. 1993. Ovine microsatellites at the OarFCB11, OarFCB128, OarFCB193, OarFCB266 and OarFCB304 loci. *Animal Genetics* 24:145–145.
- Chapuis, M.-P., and A. Estoup. 2007. Microsatellite Null Alleles and Estimation of Population Differentiation. *Molecular Biology and Evolution* 24:621–631.
- Corander, J., P. Marttinen, J. Sirén, and J. Tang. 2008. Enhanced Bayesian modelling in BAPS software for learning genetic structures of populations. *BMC Bioinformatics* 9:539.

- Coulon, A., J. F. Cosson, J. M. Angibault, B. Cargnelutti, M. Galan, N. Morellet, E. Petit, S. Aulagnier, and A. J. M. Hewison. 2004. Landscape connectivity influences gene flow in a roe deer population inhabiting a fragmented landscape: an individual-based approach. *Molecular Ecology* 13:2841–2850.
- Courbin, N., D. Fortin, C. Dussault, and R. Courtois. 2009. Landscape management for woodland caribou: the protection of forest blocks influences wolf-caribou co-occurrence. *Landscape Ecology* 24:1375–1388.
- Courtois, R., A. Gingras, D. Fortin, A. Sebbane, B. Rochette, and L. Breton. 2008. Demographic and behavioural response of woodland caribou to forest harvesting. *Canadian Journal of Forest Research* 38:2837–2849.
- De Meeûs, T. 2018. Revisiting FIS, FST, Wahlund Effects, and Null Alleles. *Journal of Heredity* 109:446–456.
- Dyer, R. J. 2014. gstudio: An R package for the spatial analysis of population genetic data.
- Emel, S. L., D. H. Olson, L. L. Knowles, and A. Storfer. 2019. Comparative landscape genetics of two endemic torrent salamander species, *Rhyacotriton kezeri* and *R. variegatus*: implications for forest management and species conservation. *Conservation Genetics* 20:801–815.
- Environment Canada. 2012. Recovery strategy for the Woodland Caribou (*Rangifer Tarandus* Caribou), boreal population, in Canada. Environment Canada, Ottawa, Ontario.
- Environment Canada. 2020. Canadian Climate Normals.
- Evanno, G., S. Regnaut, and J. Goudet. 2005. Detecting the number of clusters of individuals using the software STRUCTURE: a simulation study. *Molecular Ecology* 14:2611–2620.
- Ferguson, S. H., and P. C. Elkie. 2004. Seasonal movement patterns of woodland caribou (*Rangifer tarandus caribou*). *Journal of Zoology* 262:125–134.
- Ferguson, S. H., and P. C. Elkie. 2005. Use of Lake Areas in Winter by Woodland Caribou. *Northeastern Naturalist* 12:45–66.
- Fortin, D., R. Courtois, P. Etcheverry, C. Dussault, and A. Gingras. 2008. Winter selection of landscapes by woodland caribou: behavioural response to geographical gradients in habitat attributes. *Journal of Applied Ecology* 45:1392–1400.
- Fournier, C. n.d. Genetic networks to investigate structure and connectivity of caribou at multiple spatial and temporal scales.
- Francis, R. M. 2017. POPHELPER : an R package and web app to analyse and visualize population structure. *Molecular Ecology Resources* 17:27–32.
- François, O., and E. Durand. 2010. Spatially explicit Bayesian clustering models in population genetics. *Molecular Ecology Resources* 10:773–784.
- Frankham, R., J. Ballou, and D. A. Briscoe. 2010. Genetic Diversity. Pages 41–65 *in*. *Introduction to Conservation Genetics*. Cambridge University Press, New York.

- Frantz, A. C., S. Cellina, A. Krier, L. Schley, and T. Burke. 2009. Using spatial Bayesian methods to determine the genetic structure of a continuously distributed population: clusters or isolation by distance? *Journal of Applied Ecology* 46:493–505.
- Fryxell, J. M., T. Avgar, B. Liu, J. A. Baker, A. R. Rodgers, J. Shuter, I. D. Thompson, D. E. B. Reid, A. M. Kittle, A. Mosser, S. G. Newmaster, T. D. Nudds, G. M. Street, G. S. Brown, and B. Patterson. 2020. Anthropogenic Disturbance and Population Viability of Woodland Caribou in Ontario. *The Journal of Wildlife Management* 84:636–650.
- Galpern, P., M. Manseau, P. Hettinga, K. Smith, and P. Wilson. 2012*a*. ALLELEMATCH: an R package for identifying unique multilocus genotypes where genotyping error and missing data may be present. *Molecular Ecology Resources* 12:771–778.
- Galpern, P., M. Manseau, and P. Wilson. 2012*b*. Grains of connectivity: analysis at multiple spatial scales in landscape genetics. *Molecular Ecology* 21:3996–4009.
- Galpern, P., P. R. Peres-Neto, J. Polfus, and M. Manseau. 2014. MEMGENE: Spatial pattern detection in genetic distance data. O. Pybus, editor. *Methods in Ecology and Evolution* 5:1116–1120.
- Globus. 2007. Globus Personal Connect. <<https://www.globus.org>>. Accessed 13 Jul 2025.
- Goslee, S. C., and D. L. Urban. 2007. The **ecodist** Package for Dissimilarity-based Analysis of Ecological Data. *Journal of Statistical Software* 22.
- Goudet, J. 2005. HIERFSTAT , a package for R to compute and test hierarchical F -statistics. *Molecular Ecology Notes* 5:184–186.
- Guillot, G., R. Leblois, A. Coulon, and A. C. Frantz. 2009. Statistical methods in spatial genetics. *Molecular Ecology* 18:4734–4756.
- Hardy, O. J. 2003. Estimation of pairwise relatedness between individuals and characterization of isolation-by-distance processes using dominant genetic markers. *Molecular Ecology* 12:1577–1588.
- Hijmans. 2020. Terra: Spatial Data Analysis. <<https://github.com/rspsatial/terra>>.
- Hillman, S. S., R. C. Drewes, M. S. Hedrick, and T. V. Hancock. 2014. Physiological vagility and its relationship to dispersal and neutral genetic heterogeneity in vertebrates. *Journal of Experimental Biology* 217:3356–3364.
- Hornseth, M. L., and R. S. Rempel. 2016. Seasonal resource selection of woodland caribou (*Rangifer tarandus caribou*) across a gradient of anthropogenic disturbance. *Canadian Journal of Zoology* 94:79–93.
- Joly, K., B. W. Dale, W. B. Collins, and L. G. Adams. 2003. Winter habitat use by female caribou in relation to wildland fires in interior Alaska. *Canadian Journal of Zoology* 81:1192–1201.
- Jombart, T. 2008. *adeget* : a R package for the multivariate analysis of genetic markers. *Bioinformatics* 24:1403–1405.

- Kalisz, S., J. D. Nason, F. M. Hanzawa, and S. J. Tonsor. 2001. SPATIAL POPULATION GENETIC STRUCTURE IN TRILLIUM GRANDIFLORUM: THE ROLES OF DISPERSAL, MATING, HISTORY, AND SELECTION. *Evolution* 55:1560–1568.
- Kamvar, Z. N., J. F. Tabima, and N. J. Grünwald. 2014. *Poppr*: an R package for genetic analysis of populations with clonal, partially clonal, and/or sexual reproduction. *PeerJ* 2:e281.
- Keck, F., T. Peller, R. Alther, C. Barouillet, R. Blackman, E. Capo, T. Chonova, M. Couton, L. Fehlinger, D. Kirschner, M. Knüsel, L. Muneret, R. Oester, K. Tapoleczai, H. Zhang, and F. Altermatt. 2025. The global human impact on biodiversity. *Nature* 641:395–400.
- Keim, J. L., P. D. DeWitt, S. F. Wilson, J. J. Fitzpatrick, N. S. Jenni, and S. R. Lele. 2021. Managing animal movement conserves predator–prey dynamics. *Frontiers in Ecology and the Environment* 19:379–385.
- Keyghobadi, N. 2007. The genetic implications of habitat fragmentation for animals This review is one of a series dealing with some aspects of the impact of habitat fragmentation on animals and plants. This series is one of several virtual symposia focussing on ecological topics that will be published in the Journal from time to time. *Canadian Journal of Zoology* 85:1049–1064.
- Konkolics, S., M. Dickie, R. Serrouya, D. Hervieux, and S. Boutin. 2021. A Burning Question: What are the Implications of Forest Fires for Woodland Caribou? *The Journal of Wildlife Management* 85:1685–1698.
- Leblond, M., M.-H. St-Laurent, and S. D. Côté. 2016. Caribou, water, and ice – fine-scale movements of a migratory arctic ungulate in the context of climate change. *Movement Ecology* 4.
- Lelotte, L., M. Panzacchi, C. A. Johnson, A. Myserud, B. B. Hansen, B. B. Niebuhr, M. S. Boyce, A. Stien, E. H. Merrill, C. M. Rolandsen, T. Tveraa, V. Gundersen, and B. Van Moorter. 2025. Population and habitat assessments for conservation: Comparing national strategies for Canadian boreal caribou and Norwegian wild reindeer. *Global Ecology and Conservation* 61:e03668.
- Manel, S., and R. Holderegger. 2013. Ten years of landscape genetics. *Trends in Ecology & Evolution* 28:614–621.
- Manel, S., M. K. Schwartz, G. Luikart, and P. Taberlet. 2003. Landscape genetics: combining landscape ecology and population genetics. *Trends in Ecology & Evolution* 18:189–197.
- McFarlane, S., M. Manseau, T. B. Jones, D. Pouliot, G. Mastro Monaco, G. Pittoello, and P. J. Wilson. 2022. Identification of familial networks reveals sex-specific density dependence in the dispersal and reproductive success of an endangered ungulate. *Frontiers in Ecology and Evolution* 10:956834.
- McLoughlin, P. D., D. Paetkau, M. Duda, and S. Boutin. 2004. Genetic diversity and relatedness of boreal caribou populations in western Canada. *Biological Conservation* 118:593–598.
- Mcrae, B. H. n.d. Isolation by Resistance.

- McRae, B. H., B. G. Dickson, T. H. Keitt, and V. B. Shah. 2008. Using circuit theory to model connectivity in ecology, evolution, and conservation. *Ecology* 89:2712–2724.
- Meirmans, P. G. 2012. The trouble with isolation by distance. *Molecular Ecology* 21:2839–2846.
- MNRF. 2014. Integrated Range Assessment for Woodland Caribou and their Habitat - Churchill Range 2012.
- Moore, S. S., W. Barendse, K. T. Berger, S. M. Armitage, and D. J. Hetzel. 1992. Bovine and ovine DNA microsatellites from the EMBL and GENBANK databases. *Animal Genetics* 23:463–467.
- Mumma, M. A., M. P. Gillingham, C. J. Johnson, and K. L. Parker. 2019. Functional responses to anthropogenic linear features in a complex predator-multi-prey system. *Landscape Ecology* 34:2575–2597.
- Ontario. 2024. GeoHub: Ontario’s geospatial open data portal. <<https://geohub.lio.gov.on.ca/>>.
- Palm, E. C., E. L. Landguth, Z. A. Holden, C. C. Day, C. T. Lamb, P. F. Frame, A. T. Morehouse, G. Mowat, M. F. Proctor, M. A. Sawaya, G. Stenhouse, J. Whittington, and K. A. Zeller. 2023. Corridor-based approach with spatial cross-validation reveals scale-dependent effects of geographic distance, human footprint and canopy cover on grizzly bear genetic connectivity. *Molecular Ecology* 32:5211–5227.
- Paradis, E. 2010. pegas: an R package for population genetics with an integrated–modular approach. *Bioinformatics* 26:419–420.
- Peterman, W. E. 2018. ResistanceGA: An R package for the optimization of resistance surfaces using genetic algorithms. *Methods in Ecology and Evolution* 9:1638–1647.
- Priadka, P., M. Manseau, T. Trottier, D. Hervieux, P. Galpern, P. D. McLoughlin, and P. J. Wilson. 2019a. Partitioning drivers of spatial genetic variation for a continuously distributed population of boreal caribou: Implications for management unit delineation. *Ecology and Evolution* 9:141–153.
- Priadka, P., M. Manseau, T. Trottier, D. Hervieux, P. Galpern, P. D. McLoughlin, and P. J. Wilson. 2019b. Partitioning drivers of spatial genetic variation for a continuously distributed population of boreal caribou: Implications for management unit delineation. *Ecology and Evolution* 9:141–153.
- Pritchard, J. K., M. Stephens, and P. Donnelly. 2000. Inference of Population Structure Using Multilocus Genotype Data. *Genetics* 155:945–959.
- Racey, G., A. Harris, L. Gerrish, T. Armstrong, J. Baker, and J. McNicol. 1999. Forest Management Guidelines for the conservation of Woodland Caribou.
- Rettie, W. J., and F. Messier. 2000. Hierarchical habitat selection by woodland caribou: its relationship to limiting factors. *Ecography* 23:466–478.
- Rivera-Ortíz, F. A., R. Aguilar, M. D. C. Arizmendi, M. Quesada, and K. Oyama. 2015. Habitat fragmentation and genetic variability of tetrapod populations. *Animal Conservation* 18:249–258.

- Ruiz-Gonzalez, A., S. A. Cushman, M. J. Madeira, E. Randi, and B. J. Gómez-Moliner. 2015. Isolation by distance, resistance and/or clusters? Lessons learned from a forest-dwelling carnivore inhabiting a heterogeneous landscape. *Molecular Ecology* 24:5110–5129.
- Sexton, J. P., M. Clemens, N. Bell, J. Hall, V. Fyfe, and A. A. Hoffmann. 2024. Patterns and effects of gene flow on adaptation across spatial scales: implications for management. *Journal of Evolutionary Biology* 37:732–745.
- Shah, V. B., and B. H. McRae. 2008. Circuitscape: A tool for landscape ecology. *Proceedings of the 7th Python in Science Conference (SciPy2008)*.
- Shirk, A. J., and S. A. Cushman. 2011. sGD: software for estimating spatially explicit indices of genetic diversity. *Molecular Ecology Resources* 11:922–934.
- Shirk, A. J., E. L. Landguth, and S. A. Cushman. 2017. A comparison of individual-based genetic distance metrics for landscape genetics. *Molecular Ecology Resources* 17:1308–1317.
- Sork, V. L., and L. Waits. 2010. Contributions of landscape genetics – approaches, insights, and future potential. *Molecular Ecology* 19:3489–3495.
- Stuart-Smith, A. K., C. J. A. Bradshaw, S. Boutin, D. M. Hebert, and A. B. Rippin. 1997. Woodland Caribou Relative to Landscape Patterns in Northeastern Alberta. *The Journal of Wildlife Management* 61:622.
- Tatham, S. 1996. PuTTY. <chiark.greenend.org.uk/~sgtatham/putty/latest.html>.
- Thermo Fisher Scientific. 2023. Nanodrop One Spectrophotometer User Guide.
- Thompson, L. M., C. F. C. Klütsch, M. Manseau, and P. J. Wilson. 2019. Spatial differences in genetic diversity and northward migration suggest genetic erosion along the boreal caribou southern range limit and continued range retraction. *Ecology and Evolution* 9:7030–7046.
- Tracz, B. V., J. M. LaMontagne, E. M. Bayne, and S. Boutin. 2010. Annual and monthly range fidelity of female boreal woodland caribou in response to petroleum development. *Rangifer* 30:31–44.
- Vors, L. S., J. A. Schaefer, B. A. Pond, A. R. Rodgers, and B. R. Patterson. 2007. Woodland Caribou Extirpation and Anthropogenic Landscape Disturbance in Ontario. *The Journal of Wildlife Management* 71:1249–1256.
- Weckworth, B. V., M. Musiani, N. J. Decesare, A. D. McDevitt, M. Hebblewhite, and S. Mariani. 2013. Preferred habitat and effective population size drive landscape genetic patterns in an endangered species. *Proceedings of the Royal Society B: Biological Sciences* 280.
- Weir, B. S., and C. C. Cockerham. n.d. Estimating F-Statistics for the Analysis of Population Structure.
- Wickham, H. 2016. ggplot2: Elegant Graphics for Data Analysis. 2nd ed. 2016. Use R!, Springer International Publishing : Imprint: Springer, Cham.

- Wilson, G. A., C. Strobeck, L. Wu, and J. W. Coffin. 1997. Characterization of microsatellite loci in caribou *Rangifer tarandus*, and their use in other artiodactyls. *Molecular Ecology* 6:697–699.
- Wittmer, H. U., B. N. McLellan, and F. W. Hovey. 2006. Factors Influencing Variation in Site Fidelity of Woodland Caribou (*Rangifer tarandus caribou*) in southeastern British Columbia. *Canadian Journal of Zoology*.
- Wittmer, H. U., B. N. McLellan, R. Serrouya, and C. D. Apps. 2007. Changes in landscape composition influence the decline of a threatened woodland caribou population. *Journal of Animal Ecology* 76:568–579.
- Wright, S. 1943. Isolation by Distance. *Genetics* 28:114–138.
- Yannic, G., L. Pellissier, J. Ortego, N. Lecomte, S. Couturier, C. Cuyler, C. Dussault, K. J. Hundertmark, R. J. Irvine, D. A. Jenkins, L. Kolpashikov, K. Mager, M. Musiani, K. L. Parker, K. H. Røed, T. Sipko, S. G. Pórisson, B. V. Weckworth, A. Guisan, L. Bernatchez, and S. D. Côté. 2014. Genetic diversity in caribou linked to past and future climate change. *Nature Climate Change* 4:132–137.
- Yannic, G., M.-H. St-Laurent, J. Ortego, J. Taillon, A. Beauchemin, L. Bernatchez, C. Dussault, and S. D. Côté. 2016. Integrating ecological and genetic structure to define management units for caribou in Eastern Canada. *Conservation Genetics* 17:437–453.
- Yu, G. 2016. Scatterpie: Scatter Pie Plot. Accessed 13 Jul 2025.

SUPPLEMENTAL INFORMATION

Supplemental Table S1. Primer information, including loci names, size range, primer concentration (μM), 5' dye, forward and reverse primer sequences.

Locus	Size Range	Multiplex	Primer (μM)	5' Dye	Forward (5'-3')	Reverse (5'-3')	Reference
FCB193	96-124	1	0.1	NED	TTCATCTCAGACTGGGATTCAGAAAGGC	GCTTGGAAATAACCCTCCTGCATCC	(Buchanan and Crawford 1993)
BMS1788	118-148	1	0.1	PET	ATTCATATCTACGTCCAGATTCAGATTTCTTG	GGAGAGGAATCTTGCAAAGG	2
RT27	128-159	2	0.05	6FAM	CCAAAGACCCAACAGATG	TTGTAACACAGCAAAAGCATT	3
RT9	105-131	2	0.1	VIC	TGAAGTTTAATTTCCACTCT	CAGTCACTTTTCATCCCACAT	3
RT7	216-236	2	0.05	VIC	CCTGTTCTACTCTTCTTCTC	ACTTTTCACGGGCACTGGTT	3
RT5	139-169	2	0.05	NED	TGGTTGGAAGGAAAACCTGG	CCTCTGCTCCTCAAGACAC	3
MAP2C	93-115	2	0.1	PET	TTTACCAGACAGTTTAGTTTTGAGC	AAGGATTCTGTCTGATAACCACTTAG	4(Moore et al. 1992)
OheQ	254-292	3	0.1	VIC	AGACCTGATTACAATGTGTGTCAGTGAAGGTCTTC	GATGGACCCATCCAGGCAACCATCTAG	2
RT1	218-238	3	0.15	6FAM	AGGCCATATAGGAGGCAAGCTT	CATCTTCCCATCCTCTTTAC	3
BM888	172-203	3	0.5	VIC	CACTTGGCTTTTGGACTTA	CTGGTGTATGTATGCACACT	5
BM848	359-383	3	0.3	NED	TGCCTTCTTTCATCCAACAA	CATCTTCCCATCCTCTTTAC	5
RT24	203-235	3	0.15	NED	TGTATCCATCTGGAAGATTTCAG	CAGTTTAACCAGTCCTCTGTG	3
RT30	186-210	3	0.15	PET	TCAGCAATTCAGTACATCACCC	GCGCAAGTTTCCTCATGC	3

1 (Buchanan and Crawford 1993); 2 (Yannic et al. 2014); 3 (Wilson et al. 1997); 4 (Moore et al. 1992); 5 (Bishop et al. 1994)

Supplemental Table S2. Summary of multiple-predictor resistance surface models evaluated in step 2 of model selection. Each model tests a specific hypothesis about how landscape features may facilitate or impede gene flow in woodland caribou.

Model	Predicted Effect on Gene Flow	Rationale
Wetlands + Conifer	Facilitates	Combines movement through wetlands with preferred forest habitat.
Wetlands + Roads	Mixed	Roads may fragment habitat or increase predation risk, reducing gene flow.
Wetlands + Water	Mixed	Large waterbodies may act as barriers to movement in some regions.
Wetlands + Harvest	Mixed	Recently harvested areas may disrupt movement corridors and habitat use.
Wetlands + Fire	Mixed	Included to test for region-specific effects of recent natural disturbance.
Roads + Harvest	Impedes	Evaluates cumulative resistance from anthropogenic disturbance.
Wetlands + Roads + Conifer	Mixed	Tests for interaction between facilitative (wetlands, conifer) and resistive (roads) elements.
Conifer + Water	Mixed	Investigates seasonal effects of waterbodies and selection for preferred habitat
Conifer + Wetlands	Facilitates	Top single-predictor models included to test for cumulative effects
Conifer + Fire	Mixed	The region's rich history of fires may reduce the proportion of available preferred habitat
Conifer + Deciduous	Mixed	Examines canopy composition and its influence on cover and predation.
Conifer + Harvest	Mixed	Harvest may reduce suitable forest cover and fragment habitat.

Conifer + Roads	Mixed	Roads fragment habitat and may make sections of forest less accessible.
-----------------	-------	---

Supplemental Table S3. Summary of microsatellite diversity statistics for each genetic neighbourhood.

NH ID	N	A	Ap	Ar	Hs	Ho	FIS
A1S1	50	7.5	0.81	5.32	0.70	0.70	-0.0054
A11S1	30	7.1	0.77	5.42	0.71	0.72	-0.0117
A12S1	18	5.5	0.60	4.75	0.66	0.62	0.0575
A13S1	22	6.1	0.66	4.95	0.66	0.61	0.0815
A14S1	26	7.3	0.79	5.41	0.68	0.66	0.0288
A15S1	33	7.5	0.81	5.33	0.68	0.66	0.0256
A2S1	49	7.5	0.81	5.32	0.70	0.70	-0.0007
A3S1	58	7.6	0.83	5.19	0.69	0.69	0.0085
A4S1	58	7.6	0.83	5.19	0.69	0.69	0.0085
A5S1	54	7.4	0.80	5.18	0.70	0.70	-0.0023
A6S1	25	6.8	0.74	5.33	0.70	0.68	0.0389
A7S1	29	7.1	0.77	5.34	0.70	0.68	0.0373
A8S1	25	7.0	0.76	5.33	0.69	0.68	0.0270
A9S1	10	5.2	0.57	5.23	0.72	0.72	0.0151
B1S1	53	7.8	0.85	5.36	0.70	0.68	0.0286
B10S1	26	7.3	0.79	5.41	0.68	0.66	0.0288
B11S1	23	6.4	0.69	5.07	0.66	0.66	-0.0027
B2S1	49	7.5	0.81	5.32	0.70	0.70	-0.0007
B3S1	12	5.4	0.58	5.08	0.68	0.75	-0.1167
B4S1	49	7.5	0.81	5.32	0.70	0.70	-0.0007
B5S1	58	7.6	0.83	5.19	0.69	0.69	0.0085
B6S1	12	5.2	0.57	4.98	0.68	0.71	-0.0541
B8S1	11	5.8	0.63	5.63	0.72	0.69	0.0401
B9S1	18	5.9	0.64	5.00	0.66	0.66	-0.0012
C1S1	27	7.1	0.77	5.37	0.70	0.68	0.0296
C10S1	27	6.9	0.75	5.44	0.71	0.73	-0.0249
C11S1	30	6.8	0.73	5.32	0.71	0.71	0.0078
C12S1	25	6.5	0.71	5.28	0.71	0.71	0.0055
C13S1	25	6.5	0.71	5.28	0.71	0.71	0.0055
C14S1	14	5.5	0.60	5.15	0.72	0.72	0.0003
C16S12	17	5.6	0.61	4.84	0.63	0.62	0.0277
C17S1	22	6.1	0.66	4.95	0.66	0.61	0.0815
C18S1	25	6.3	0.68	5.02	0.66	0.63	0.0682
C19S1	13	5.6	0.61	5.12	0.67	0.66	0.0344
C2S1	53	7.8	0.84	5.36	0.70	0.70	0.0056
C20S1	11	5.5	0.60	5.34	0.70	0.70	0.0148
C24S1	23	6.4	0.69	5.07	0.66	0.66	-0.0027
C25S1	23	6.4	0.69	5.07	0.66	0.66	-0.0027
C26S1	20	6.1	0.66	4.99	0.65	0.65	-0.0060
C27S1	12	5.2	0.57	4.98	0.68	0.71	-0.0541
C3S4	50	7.6	0.83	5.26	0.70	0.70	-0.0058
C327	50	7.6	0.83	5.26	0.70	0.70	-0.0058
C4S10	58	7.6	0.83	5.19	0.69	0.69	0.0085
C7S10	54	7.6	0.83	5.13	0.70	0.68	0.0212
C8S1	38	6.8	0.73	4.93	0.69	0.68	-0.0021
C9S1	30	6.5	0.70	4.95	0.68	0.67	0.0063

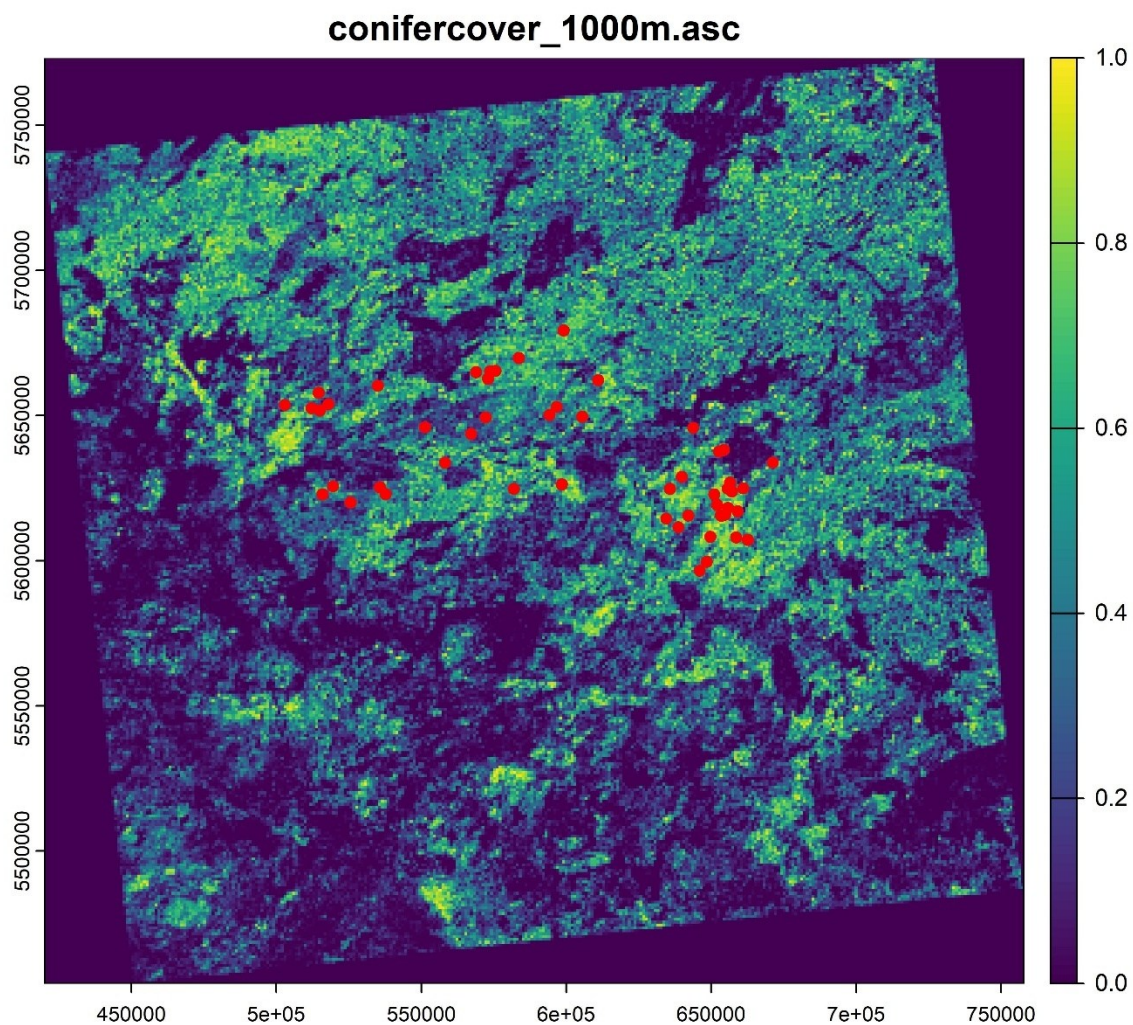
Average	31.4	6.7	0.72	5.19	0.69	0.68	0.0098
---------	------	-----	------	------	------	------	--------

NH_ID = genetic neighbourhood identifier; N = number of individuals; A = total number of alleles; A_p = number of private alleles; Ar = allelic richness (standardized for sample size); H_s = expected heterozygosity; H_o = observed heterozygosity; FIS = inbreeding coefficient.

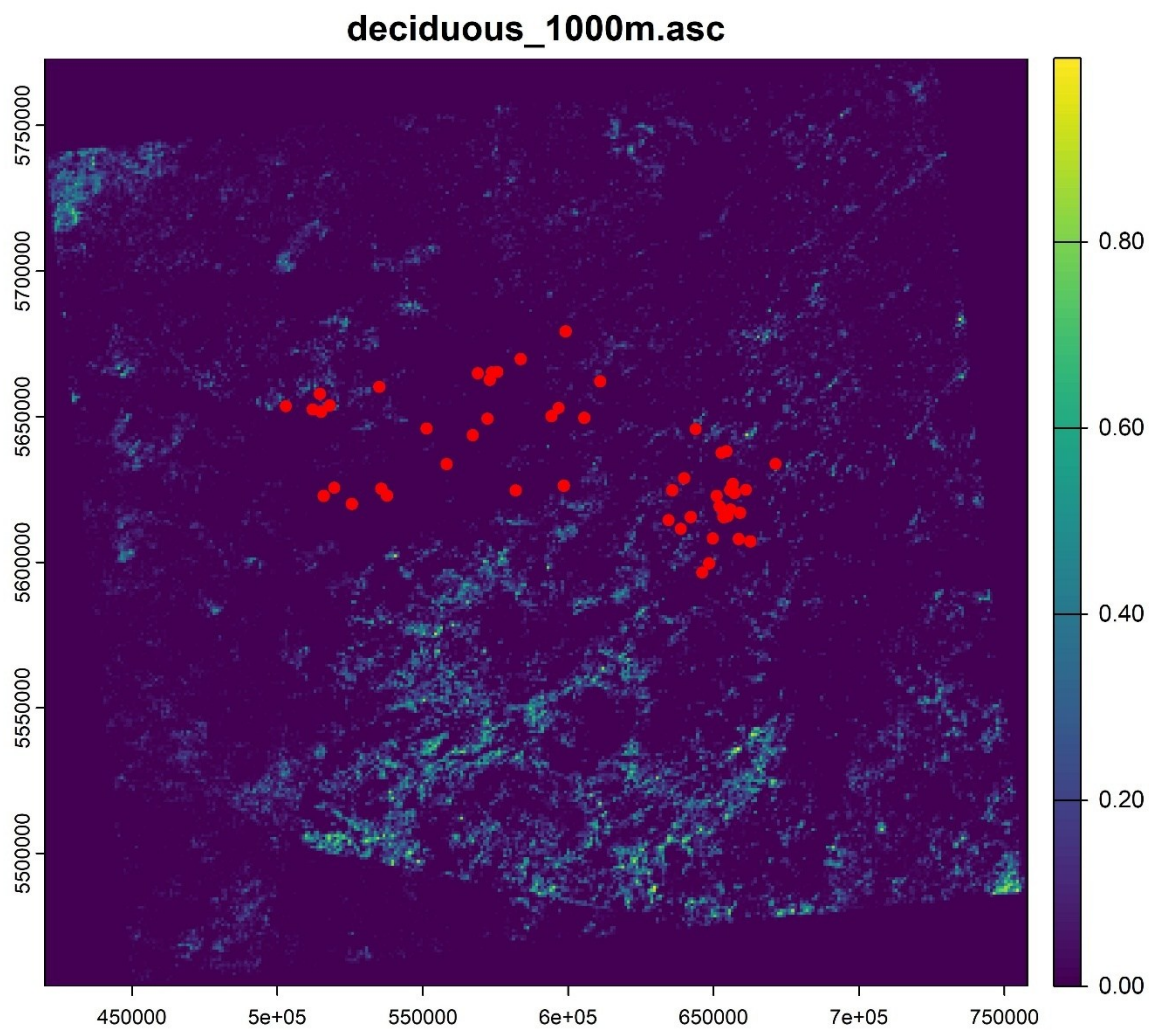
Supplemental Table S4. Summary of single-predictor resistance surface model performance for each of four genetic distance metrics. For each surface, only the top-performing replicate is reported.

Genetic Distance	Surface	k	AICc	Δ AICc	LL	Equation	Shape	Max
Fij	Conifer	4	-678836.5	0	339422.4	M	2	9.2
	Roads	4	-678831.1	5.4	339419.6	IM	0.5	3.1
	Harvest	4	-678827.9	8.6	339418.1	IM	0.6	1.1
	Fire	4	-678827.7	8.8	339418.0	IM	0.8	249.9
	Distance	2	-678827.4	9.1	339415.7	-	-	-
	Deciduous	4	-678827.3	9.2	339417.8	IM	1	11.3
	Water	4	-678825.7	10.8	339416.9	IRM	0.9	202.8
	Wetlands	4	-678825.5	11	339416.8	IM	0.5	11.6
	Null	1	-678650	186.5	339326.0	-	-	-
Dps	Wetlands	4	-70897.6	0	35452.9	IM	2	24.3
	Water	4	-70885.1	12.5	35446.6	M	2.1	89.2
	Roads	4	-70884.8	12.8	35446.5	M	0.7	237.1
	Conifer	4	-70883.7	13.9	35445.9	IRM	14.4	47.6
	Harvest	4	-70881.7	15.9	35445.0	M	0.5	38.5
	Fire	4	-70881.5	16.1	35444.8	IM	0.5	246.7
	Deciduous	4	-70876.8	20.8	35442.5	M	0.5	45.1
	Distance	2	-70876.5	21.1	35440.3	-	-	-
	Null	1	-70712.3	185.3	35357.2	-	-	-
PCA10	Wetlands	4	100917.2	0	-50454.5	IM	1.7	15.9
	Harvest	4	100933.1	15.9	-50462.5	M	2.1	128.5
	Water	4	100933.1	15.9	-50462.5	M	2.1	128.1
	Roads	4	100944.9	27.7	-50468.4	IM	0.9	28
	Conifer	4	100954.7	37.5	-50473.2	IRM	1.4	23.5
	Deciduous	4	100959.9	42.7	-50475.9	M	0.5	45.2
	Fire	4	100960.6	43.4	-50476.2	IM	0.5	8.8
	Distance	2	100967.2	50	-50481.6	-	-	-
	Null	1	101385.5	468.3	-50691.7	-	-	-
PCA64	Wetlands	4	88901.9	0	-44446.9	IM	0.6	155
	Water	4	88922	20.1	-44456.9	M	3.2	196.9
	Conifer	4	88922.8	20.9	-44457.3	IRM	12.2	161.9
	Harvest	4	88924.4	22.5	-44458.1	RM	5.8	15
	Roads	4	88925.2	23.3	-44458.5	IM	0.9	41.2
	Fire	4	88926.7	24.8	-44459.3	IM	0.5	246.9
	Deciduous	4	88936.8	34.9	-44464.3	IM	0.5	17.5
	Distance	2	88939.7	37.8	-44467.8	-	-	-
	Null	1	89124.5	222.6	-44561.2	-	-	-

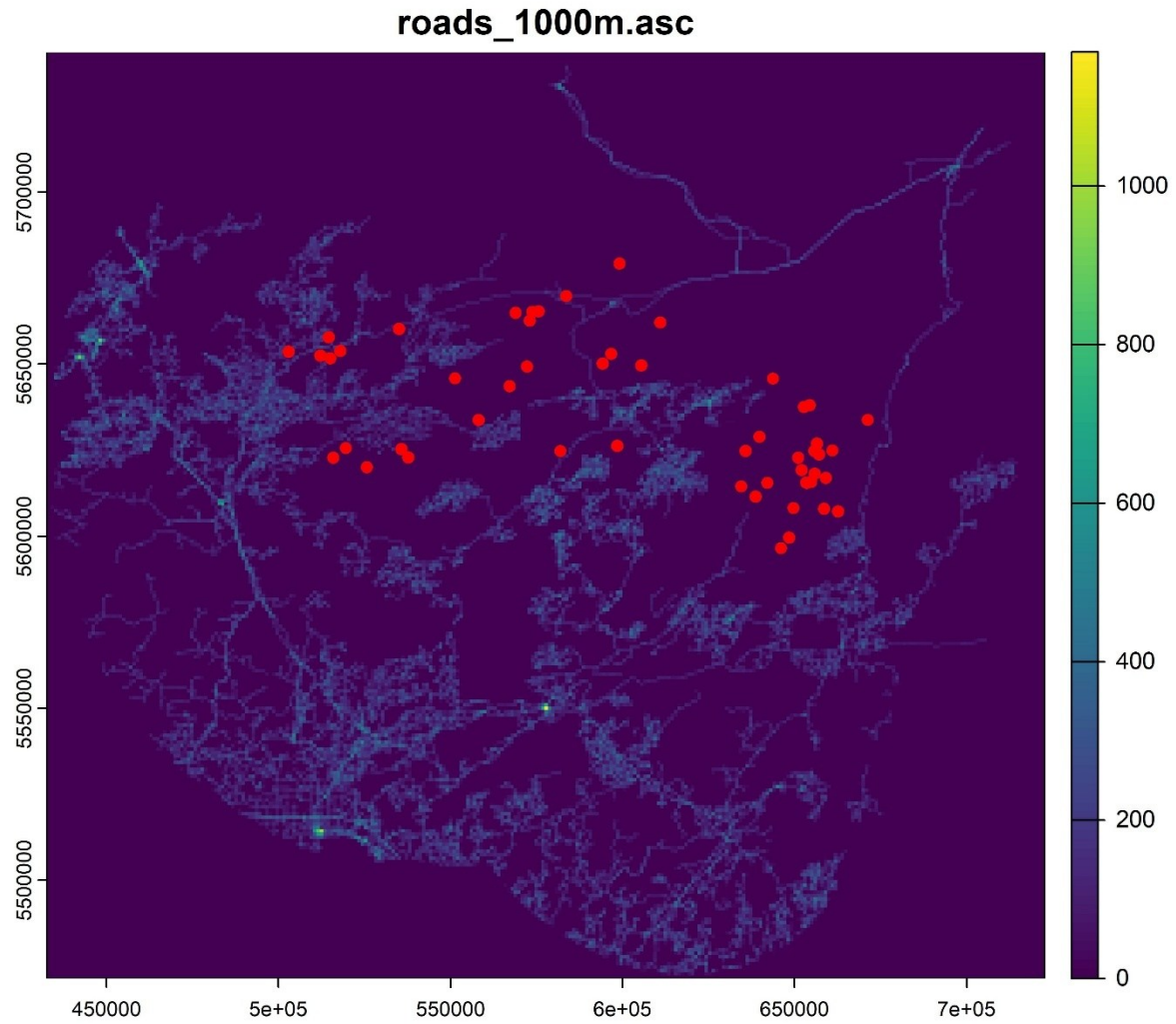
Equation refers to the transformation function applied to the resistance surface: M = monomolecular, IM = inverse monomolecular, RM = reverse monomolecular, IRM = inverse-reverse monomolecular, “-” = untransformed (e.g., distance/null models). Shape and Max are the fitted parameters for the transformation. Δ AICc values are shown relative to the top-performing model for each genetic distance metric.



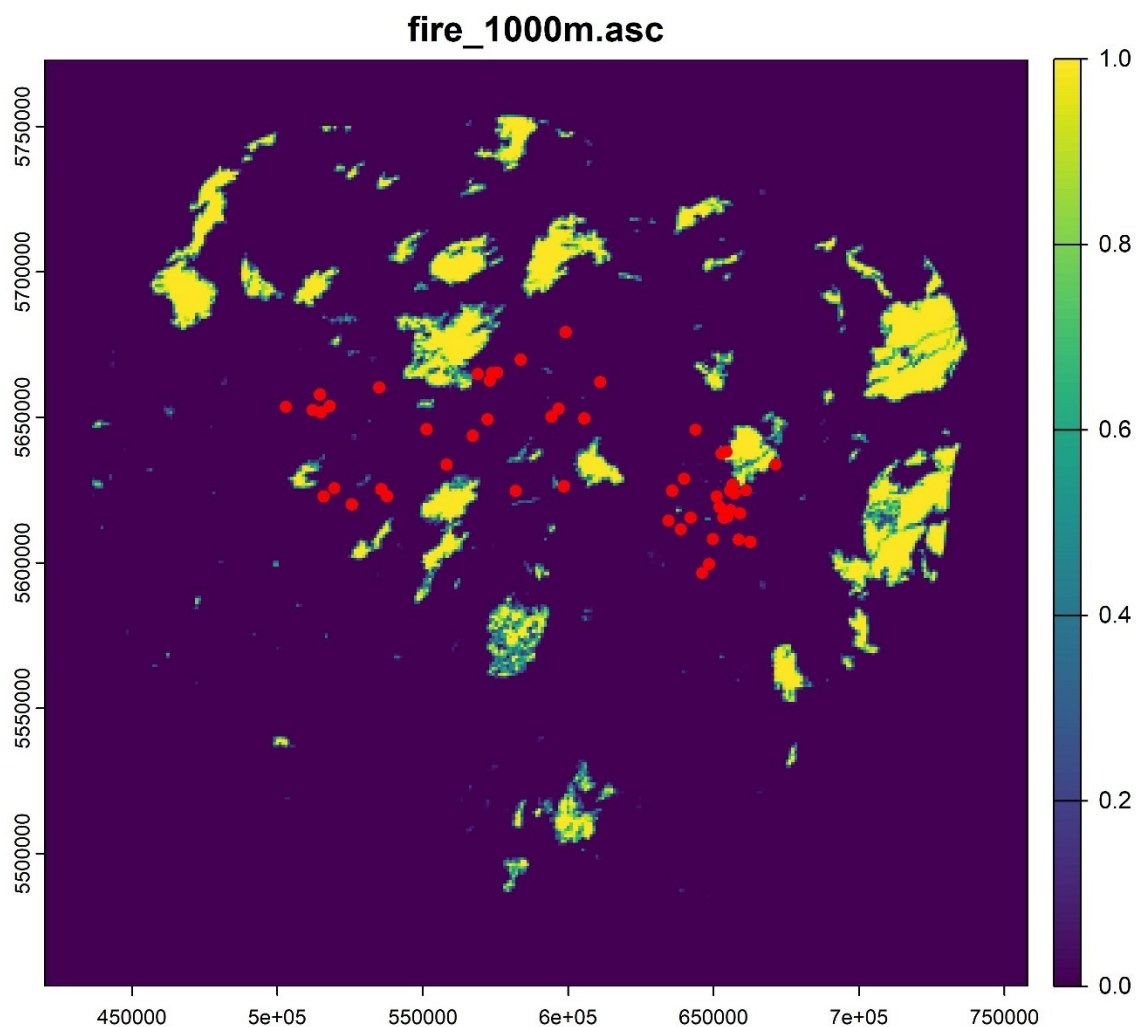
Supplemental Figure S1. Raster layer showing the proportion of conifer cover within a 1000 m moving window across the Churchill Range. Values range from 0 (absence) to 1 (complete cover). Red points indicate sampled caribou locations.



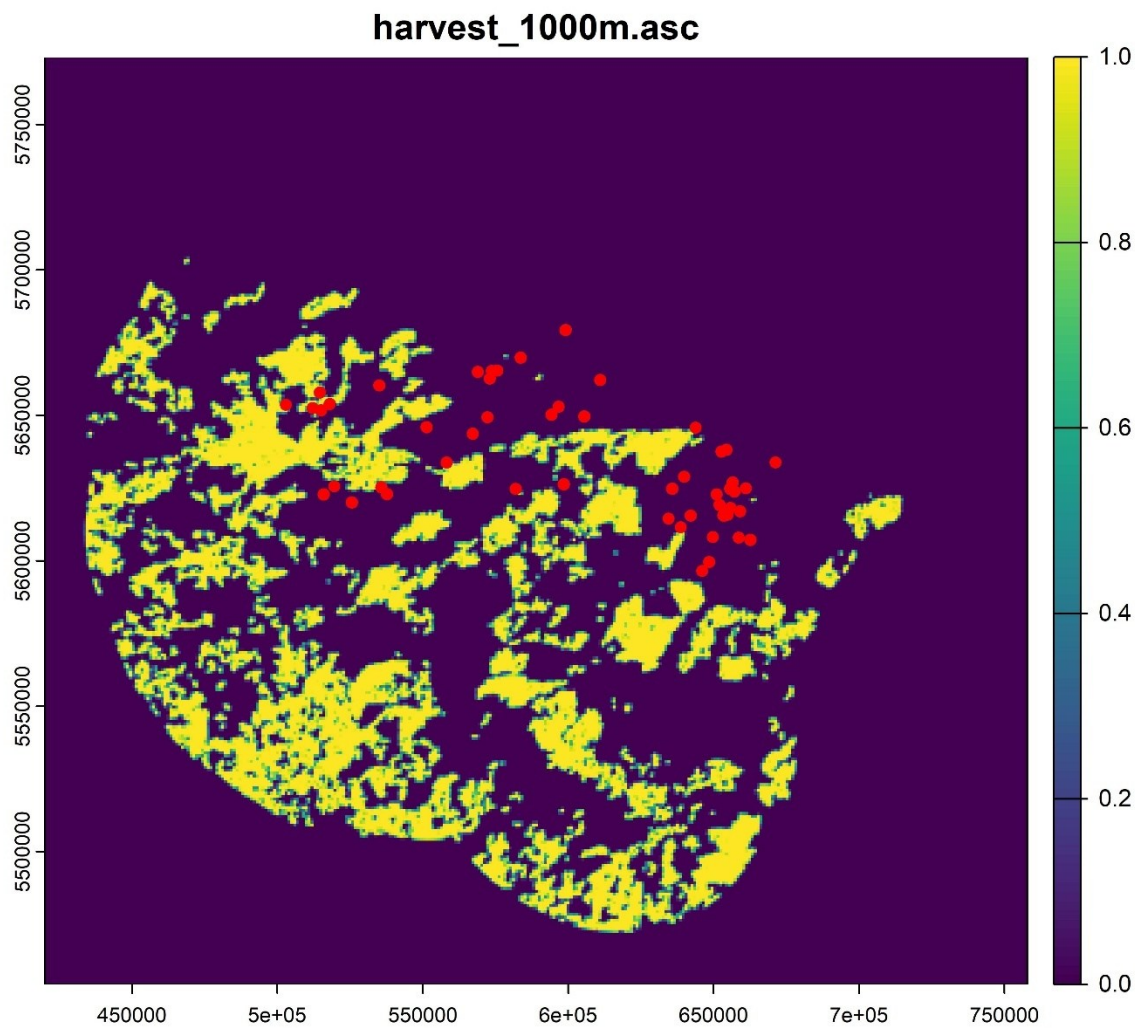
Supplemental Figure S2. Raster layer showing the proportion of deciduous cover within a 1000 m moving window across the Churchill Range. Values range from 0 (absence) to 1 (complete cover). Red points indicate sampled caribou locations.



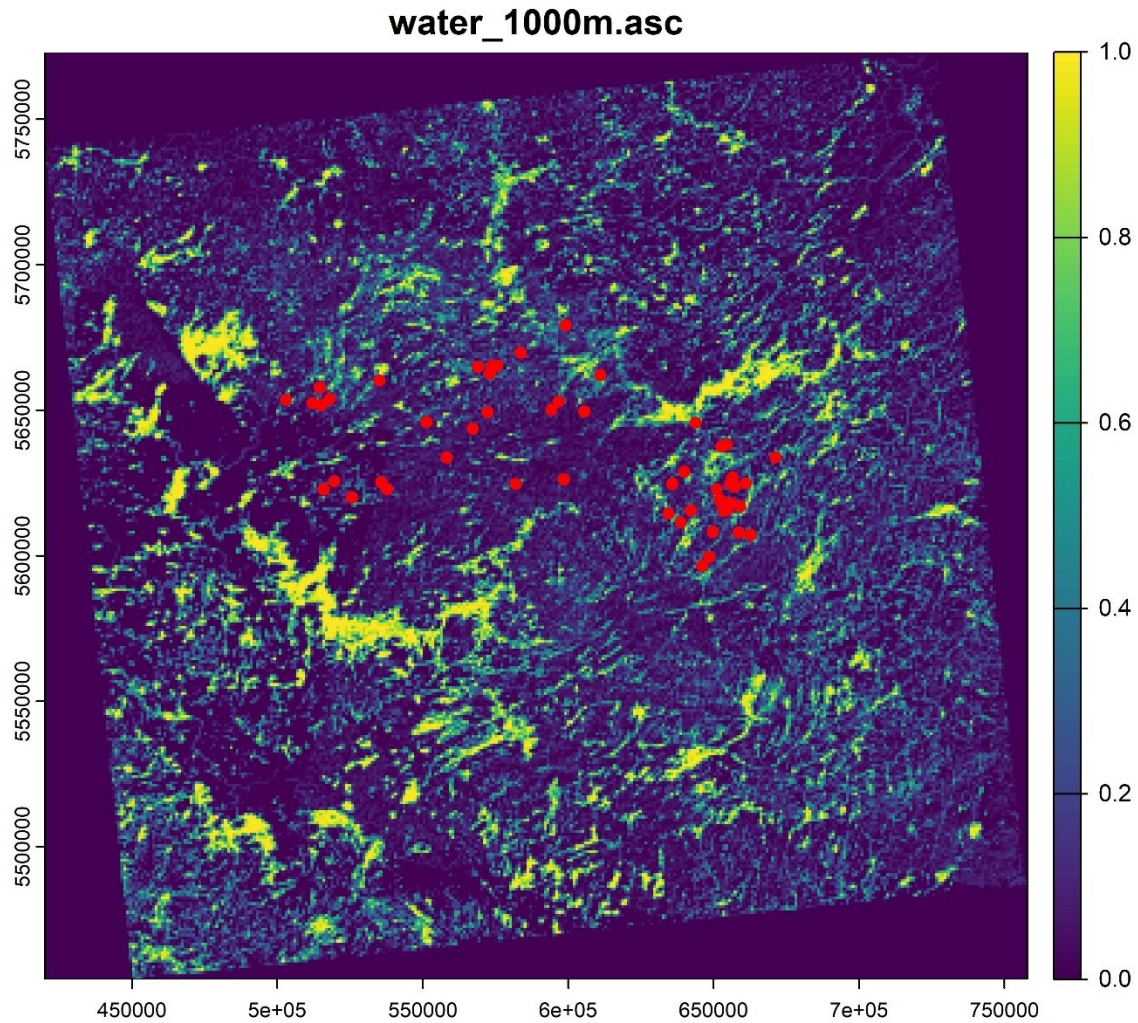
Supplemental Figure S3. Raster layer showing the network of roads across the range within a 1000 m moving window across the Churchill Range. Values range from 0 (absence) to 1 (complete cover). Red points indicate sampled caribou locations.



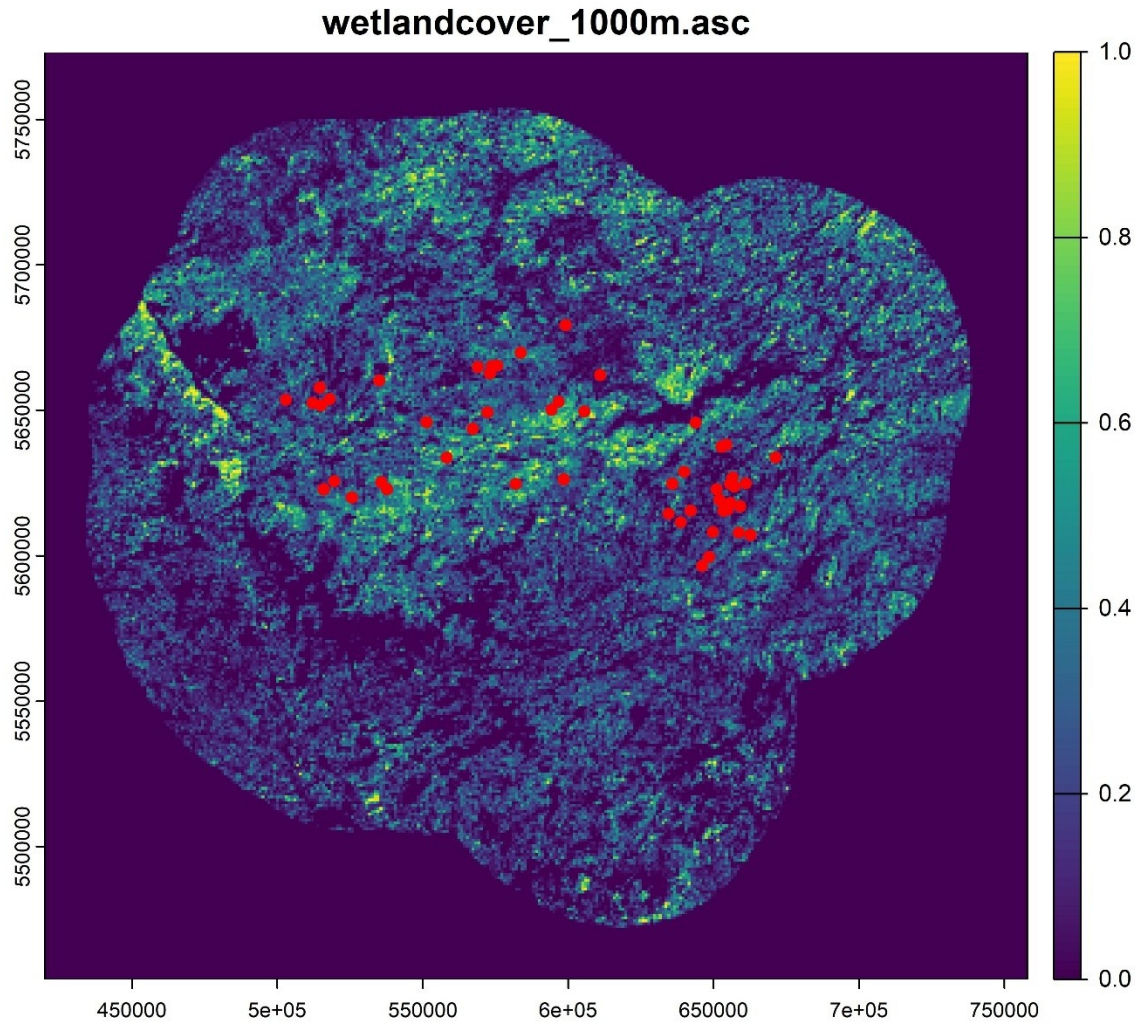
Supplemental Figure S4. Raster layer showing the proportion of fire cover within a 1000 m moving window across the Churchill Range. Values range from 0 (absence) to 1 (complete cover). Red points indicate sampled caribou locations.



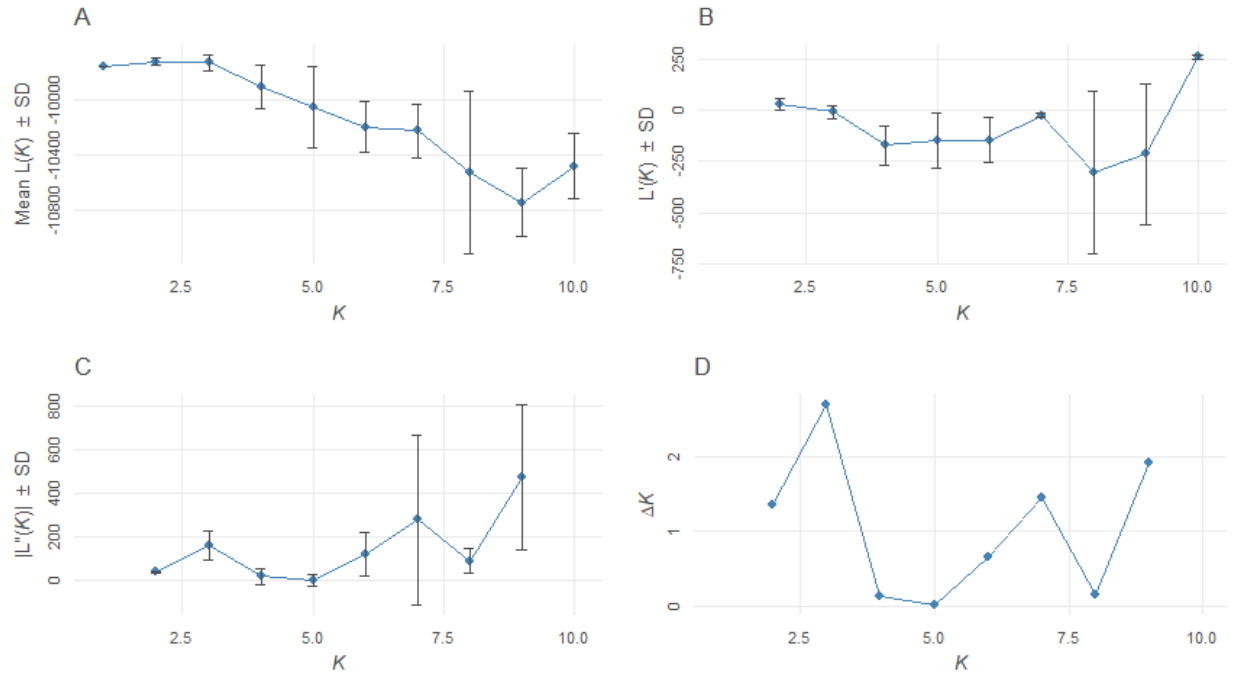
Supplemental Figure S5. Raster layer showing the proportion of conifer cover within a 1000 m moving window across the Churchill Range. Values range from 0 (absence) to 1 (complete cover). Red points indicate sampled caribou locations.



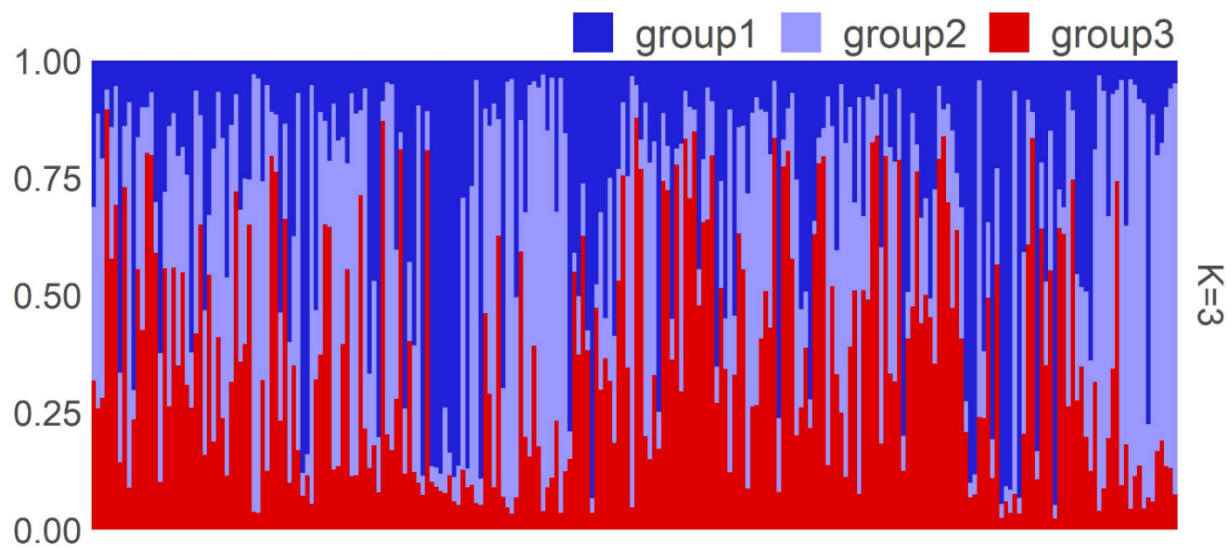
Supplemental Figure S6. Raster layer showing the proportion of waterbody cover within a 1000 m moving window across the Churchill Range. Values range from 0 (absence) to 1 (complete cover). Red points indicate sampled caribou locations.



Supplemental Figure S7. Raster layer showing the proportion of wetland cover within a 1000 m moving window across the Churchill Range. Values range from 0 (absence) to 1 (complete cover). Red points indicate sampled caribou locations.



Supplemental Figure S8. Summary statistics for STRUCTURE runs across different values of K used to determine the most likely number of genetic clusters. (A) Mean $[Ln P(K)] \pm SD$ across replicate runs for each K . (B) First-order rate of change in $Ln P(K)$ with respect to K . (C) Second-order rate of change in $Ln P(K)$, or $L''(K) \pm SD$, used in the calculation of ΔK . (D) ΔK values, which reflect the rate of change in the log likelihood between successive K values. SD = standard deviation.



Supplemental Figure S9. STRUCTURE bar plot showing individual genetic assignment probabilities for $K = 3$ genetic clusters. Each bar represents one individual, with color proportions indicating the estimated fraction of that individual's genome assigned to each cluster.